Japan Geoscience Union Meeting 2014
(28 April - 02 May 2014 at Pacifico YOKOHAMA, Kanagawa, Japan)

PEM36-01 Room:312 Time:April 28 09:00-09:15

Effect of Surface BRDF on the Geostationary and Low Orbit Observations of Tropospheric NO_2

NOGUCHI, Katsuyuki[1*] ; RICHTER, Andreas[2] ; ROZANOV, Vladimir[2] ; ROZANOV, Alexei[2] ; BURROWS, John[2] ; IRIE, Hitoshi[3] ; KITA, Kazuyuki[4]

[1]Nara Women's University, [2]University of Bremen, [3]Chiba University, [4]Ibaragi University

We investigated the effect of surface reflectance anisotropy, Bidirectional Reflectance Distribution Function (BRDF), on geostationary and low orbit satellites' retrievals of tropospheric NO_2. We first develop an empirical model of the three BRDF coefficients for each land cover type over Tokyo, and then apply the model to the calculation of land cover type dependent AMFs and BAMFs. Results show that the variability of AMF among the land types is up to several tens percent, and if we neglect the reflectance anisotropy, the difference from BRDF's AMF reaches 10% or more. The evaluation of the BAMFs calculated shows that not to consider variations in BRDF will cause large errors if the concentration of NO_2 is high close to the surface, although the importance of BRDF for AMFs decreases for large AOD.

Japan Geoscience Union Meeting 2014
(28 April - 02 May 2014 at Pacifico YOKOHAMA, Kanagawa, Japan)

PEM36-02 Room:312 Time:April 28 09:15-09:30

R&D of passive radar -Water vapor estimation with digital terrestrial broadcasting wave-

KAWAMURA, Seiji[1*] ; OHTA, Hiroki[1] ; HANADO, Hiroshi[1]

[1]National Institute of Information and Communications Technology

In general, radars retrieve some information by transmitting radio waves and by receiving their scatted echoes. On the other hand, passive radars never transmit radio waves. They retrieve some information by receiving radio waves which are transmitted by others for other purposes. Passive radars do not need new radio wave frequencies, and just consist of rather simple and low cost receivers because they do not transmit radio waves. We, National Institute of Information and Communications Technology (NICT), are developing passive radar measurement systems whose targets are environmental monitoring.

In this study, we are developing a water vapor measurement system using digital terrestrial broadcasting wave as one of passive radars. Localized heavy rain in the urban area is a social issue in these days. Water vapor is an essential parameter for weather forecast because it is a state before rain drop. And it is one of the most difficult physical quantity to measure with remote sensing technique. If we can monitor water vapor around the ground surface with precise time and spacial resolutions, the weather forecast might be able to predict the localized heavy rain.

Radio waves are delayed due to water vapor through propagation. If we can measure this time delay, water vapor can be retrieved from it. Since delay doe to water vapor is quite small, very precise (sub-nano second order) measurements are needed. Radio waves used for digital terrestrial broadcasting are modulated with OFDM, and known signals are embedded. Complex delay profiles are calculated using these known signals. Using the phase of delay profile, we can measure propagation delay with precise accuracy (pico-second order).

When we consider the accuracy with order of sub-nano seconds, phase fluctuations of local oscillators at radio tower and receivers are essential error factors. We have developed a real-time delay (phase of delay profiles) measurement system with software-defined radio technique. Using this system, we can also measure phase fluctuations of local oscillator at each TV station by just receiving radio waves. With these systems at two receiving points on the same line including the radio tower, and with synchronization between their local oscillators, we can measure water vapor between two receiving points. After proving test of estimation of water vapor, we will distribute many small receivers and develop water vapor monitoring system in collaboration with many observations and data assimilations.

Keywords: passive radar, digital terrestrial broadcasting wave, water vapor, propagation delay

Japan Geoscience Union Meeting 2014
(28 April - 02 May 2014 at Pacifico YOKOHAMA, Kanagawa, Japan)

PEM36-03 Room:312 Time:April 28 09:30-09:45

Observation of local circulation in north area of Fukui prefecture by using two adjoining 1.3-GHz wind profiler radars

NAKAJO, Tomoyuki[1*] ; YAMAMOTO, Masayuki[2] ; AOYAMA, Takashi[1] ; HASHIGUCHI, Hiroyuki[2] ; UJIHASHI, Yasuyuki[3]

[1]Department of Electrical, Electronic and Computer Engineering, Fukui University of Technology, [2]Research Institute for Sustainable Humanosphere, Kyoto University, [3]Department of Architecture and Environmental Engineering, Fukui University of Technology

Global impact of our lifestyle to our own has been pointed out previously. In the field of atmospheric environment, it has been considered that heavy rainfall, of which occurrence and damages are increasing in recent years, to be related with global warming. In addition to influence of yellow dust and PM 2.5 on our health, it has been known that photochemical oxidant tends to increase again since 1980's. Furthermore, the severe accident of Fukushima Daiichi Nuclear Power Station has caused us the interest about diffusion of radioactivity.

Above atmospheric problems are not only global but also local because they are strongly affected by local circulation. Local circulation occurs in atmospheric boundary layer (ABL) which has different characteristics in each local area, therefore, it is essential to reveal the detailed characteristics of ABL for resolution of the atmospheric problems.

Under such a situation, Fukui University of Technology started a project named as "Formation of research base for measurement and conservation of environment in Hokuriku area" (H23 - H27) supported by MEXT. In the project, a 1.3-GHz wind profiler radar (FUT-WPR), which is same type atmospheric radar as that of JMA WINDAS network, was installed in the coastal area of northern part of Fukui prefecture in 2012. In Fukui prefecture, a WPR of WINDAS has worked at Fukui local meteorological observatory (WINDAS-FUKUI), and the distance between FUT-WPR and WINDAS-FUKUI is only 24 km. There is no area in Japan where two WPRs are located within such a short distance, which enables more detailed study of the local circulation in Fukui plain than previous studies.

The observation results of FUT-WPR have revealed the detailed characteristics of see and land breeze (SLB) which is well known local circulation in coastal areas; its temporal variation, structure in altitude, relation with ABL, occurrence probability, and effect on generating area of clouds. Especially, the comparison with WINDAS-FUKUI not only confirms the observation results by FUT-WPR but also shows the SLB reaches from the seashore to a few 10 km inland. Although the observation results are fundamental in meteorology, this is the first time that the real picture of SLB in Fukui plain was revealed in detail so far. The comparison with WINDAS-FUKUI also shows the horizontal winds under about 1 km in altitude often differs between FUT-WPR and WINDAS-FUKUI, which indicates the importance of measurement of ABL.

We also carried out the data analyses in the case of heavy rain. On September 3 in 2013, passage of the stationary front accompanying the typhoon No. 17 brought about the heavy rain reaching to 10 mm/10min in Fukui prefecture from 14:00 to 16:00 (JST). FUT-WPR observed not only a typical structure and temporal variation of horizontal wind followed by the passage of stationary front but also intermittent upward flow, of which velocity reaches 1 m/s in the altitude from 200 m to about 4 km, from 7 hours before the passage of front. Especially, a strong upward flow with the velocity of 4 m/s was observed around 12:00 in the altitude from 3.5 to 5 km although the duration was relatively short. The observations of MTSAT from 10:00 to 14:00 have shown that optically thick clouds, of which top altitude was estimated to reach about 10 km, had arrived over Fukui prefecture. Therefore, the upward flows observed by FUT-WPR should be a part of cumulonimbi system which brought about the heavy rain. On the other hand, upward flows observed by WINDAS-FUKUI was weaker than that of FUT-WPR, which indicates the horizontal scale of upward flow accompanying the cumulonimbi system was under 24 km at least.

The results of observations and data analyses obtained so far indicates the observation of ABL by adjoining WPRs will be useful in early detection of arriving cumulonimbi system or local weather prediction.

Keywords: atmospheric boundary layer, local circulation, see and land breeze, heavy rain, wind profiler radar

Japan Geoscience Union Meeting 2014
(28 April - 02 May 2014 at Pacifico YOKOHAMA, Kanagawa, Japan)

PEM36-04 Room:312 Time:April 28 09:45-10:00

Relationship between solar activity and disturbance in the middle atmosphere during Arctic winter

SAKANOI, Kazuyo[1*] ; KINOSHITA, Takenari[2] ; MURAYAMA, Yasuhiro[2]

[1]Komazawa Univ., [2]National Institude of Information and Communications Technology

Purpose of this research is to clarify relationship between solar activity and disturbance in the middle atmosphere during Arctic winter. In this research we consider stratospheric sudden warming (SSW), which is typical phenomenon in Arctic winter, as disturbance in the middle atmosphere including the mesosphere. Previous research reported effect of 11-year solar cycle on thermal structure only in the Stratosphere.

To get thing started, we selected daily bottom altitude of easterly wind area, which corresponds to SSW, in the zonal mean horizontal wind. Averaged value of those during one SSW event is used for quantitative comparison with solar activity and QBO index. No clear relationship was found between the selected new value (ZEW index) and two indexes. However we confirm that the ZEW index represents well the degree of disturbance. Next, we calculate AO index in the altitude range from 1000 hPa to 0.1 hPa (65km alt). AO index also represents the degree of disturbance.

In this presentation, we will examine and discuss in more detail about ZEW and AO index as those which indicate the degree of disturbance in the middle atmosphere for quantitative comparison with solar activity.

Keywords: Middle atmosphere disturbance, Solar activity, Arctic Oscillation, QBO, Arctic region, Stratospheric sudden warming

Japan Geoscience Union Meeting 2014
(28 April - 02 May 2014 at Pacifico YOKOHAMA, Kanagawa, Japan)

PEM36-05 Room:312 Time:April 28 10:00-10:15

Temporal variations of O3 and NO in the middle atmosphere above Syowa Station observed by a millimeter-wave radiometer

OHYAMA, Hirofumi[1*] ; ISONO, Yasuko[1] ; UEMURA, Miku[1] ; NAGAHAMA, Tomoo[1] ; MIZUNO, Akira[1] ; TSUTSUMI, Masaki[2] ; EJIRI, Mitsumu[2] ; NAKAMURA, Takuji[2]

[1]Solar-Terrestrial Environmental Laboratory, Nagoya University, [2]National Institute of Polar Research

Precipitation of energetic particle into the atmosphere impacts abundances of atmospheric constituents in the middle atmosphere. Highly energetic solar protons, which directly enter the middle atmosphere, cause increase of HOx and NOx species. Energetic electrons also increase NOx in the thermosphere, and the downward transport in the polar vortex moves the produced NOx to lower altitudes. These NOx species cause a decrease of O_3 in the middle atmosphere through catalytic reactions [Seppälä et al. 2006; Daae et al., 2012]. To investigate the effect of NOx on O_3 variation in the polar region, a ground-based millimeter-wave spectroscopic radiometer was installed at Syowa Station, Antarctica in March 2011. The instrument has recorded brightness temperature spectra of rotational emission from the atmospheric O_3 and NO molecules. From the NO spectra, both multiple short-term enhancements and seasonal variation of NO column are observed [Isono et al., 2014]. The short-term enhancements are correlated with the energetic particle precipitation. In the present study, O_3 profiles are retrieved from the brightness temperature spectra between 238.94-239.24 GHz, whose spectral range has sensitivity to the O_3 abundance between 20 and 70 km. The optimal estimation scheme is used for the O_3 profile retrieval, along with radiative transfer calculation through the use of the NCEP reanalysis data and spectroscopic parameters. Since the O_3 spectra are integrated over 1 hour every 6 hours, we usually derive four O_3 profiles in a day. We present the result of O_3 retrieval and discuss how the O_3 mixing ratios at given altitudes response to the short-term NO column enhancement.

Keywords: ozone, nitric oxide, remote sensing

Japan Geoscience Union Meeting 2014
(28 April - 02 May 2014 at Pacifico YOKOHAMA, Kanagawa, Japan)

PEM36-06 Room:312 Time:April 28 10:15-10:30

Current status of Syowa lidar project in the prioritized observation project for VIII-th term JARE

EJIRI, Mitsumu K.[1*] ; TSUDA, Takuo[1] ; NISHIYAMA, Takanori[1] ; ABO, Makoto[2] ; TOMIKAWA, Yoshihiro[1] ; SUZUKI, Hidehiko[3] ; KAWAHARA, Takuya[4] ; TSUTSUMI, Masaki[1] ; NAKAMURA, Takuji[1]

[1]National Institute of Polar Research, [2]Graduate School of System Design, Tokyo Metropolitan University, [3]College of Science, Rikkyo university, [4]Faculty of Engineering, Shinshu University

The National Institute of Polar Research (NIPR) is leading a six year prioritized project of the Antarctic research observations since 2010. One of the sub-project is entitled ”the global environmental change revealed through the Antarctic middle and upper atmosphere”. Profiling dynamical parameters such as temperature and wind, as well as minor constituents is the key component of observations in this project, together with a long term observations using existent various instruments in Syowa, Antarctica (69S, 39E). As a part of the sub-project, Rayleigh/Raman lidar was installed at Syowa Station in January, 2011 and has been operated at more than 350 nights (>3000 hours clear sky) by February, 2014. The Rayleigh/Raman lidar observes temperature and clouds in the mesosphere, the stratosphere and part of the troposphere, and providing seasonal and yearly variations of temperature profiles and data of gravity wave characteristics in the middle atmosphere, as well as high altitude clouds of PMC (polar mesospheric clouds) and PSC (polar stratospheric clouds). In order to extend the height coverage to include mesosphere and lower thermosphere region, and also to extend the parameters observed, a new resonance scattering lidar system with tunable wavelengths is developed at NIPR in Tachikawa (36N, 139E). The lidar transmitter is based on injection-seeded, pulsed alexandrite laser for 768-788 nm (fundamental wavelengths) and a second-harmonic generation (SHG) unit for 384-394 nm (second harmonic wavelengths). The laser wavelengths are tuned in to the resonance wavelengths by a wavemeter that is well calibrated using a wavelength-stabilized He-Ne laser. The new lidar has capabilities to measure density variations of minor constituents such as atomic iron (Fe, 386 nm), atomic potassium (K, 770 nm), calcium ion (Ca^+, 393 nm), and aurorally excited nitrogen ion ($N_2{}^+$, 390-391 nm) and temperature profiles in the mesosphere and lower thermosphere (MLT) region using resonance scatter of K. Currently, the fundamental laser pulses are transmitted with 120-160 mJ/pulse at approximately 25 Hz (i.e., $\sim$3-4 W) and the backscattered signal is received with a 35 cm diameter telescope. The new lidar system will be installed two years later at Syowa Station and provide information on the mesosphere and lower thermosphere as well as the ionosphere. This unique observation is expected to make important contribution to studies on the atmospheric vertical coupling process and the neutral and charged particle interaction. In this talk, current status of the research, observations, and system developments, as well as future plans will be presented.

Keywords: Lidar, Antarctic observation, middle and upper atmosphere, Resonance scattering, Rayleigh scattering, Raman scattering

Japan Geoscience Union Meeting 2014
(28 April - 02 May 2014 at Pacifico YOKOHAMA, Kanagawa, Japan)

PEM36-07 Room:312 Time:April 28 10:30-10:45

A daytime observation of polar mesospheric clouds with Syowa Rayleigh Raman lidar system equipped with a new etalon unit

SUZUKI, Hidehiko[1*] ; NAKAMURA, Takuji[2] ; EJIRI, Mitsumu[2] ; ABO, Makoto[3] ; YAMAMOTO, Akihiro[4] ; KAWAHARA, Taku d[4] ; TOMIKAWA, Yoshihiro[2] ; TSUTSUMI, Masaki[2] ; TSUDA, Takuo[2] ; NISHIYAMA, Takanori[2]

[1]Rikkyo University, [2]National Institute of Polar Research, [3]Tokyo Metropolitan University, [4]Shinshu University

A Rayleigh/Raman lidar system has been operated by the Japanese Antarctic Research Expedition (JARE) since February, 2011 (JARE 52nd) in Syowa Station Antarctica (69.0S, 39.5E). Polar Mesospheric Cloud (PMC) was detected by the lidar at 22:30UT (+3hr for LT) on Feb 4th, 2011, the first day of a routine operation. This event is the first time to detect PMC over Syowa Station by a lidar [Suzuki et al., 2013]. However, signal to noise ratio (SNR) of the PMC event was not so good due to a large shot noise from a daytime background signal. Moreover, a receiver system was mainly designed for nighttime observations. Therefore, observation of PMC during the midnight Sun, which also corresponds to PMC most active period, was difficult. Thus, to improve SNR of the PMC observation with Syowa Rayleigh/Raman lidar during daytime, a narrow bandpass Fabry-Perot etalon system has been developed and installed in the receiver system on Dec 2013 by JARE 55th. In this paper, Prompt report of a PMC observation with Syowa Rayleigh Raman lidar system equipped with the new etalon unit is presented.

Keywords: polar mesospheric cloud, noctilucent cloud, lidar, Antarctic

Japan Geoscience Union Meeting 2014
(28 April - 02 May 2014 at Pacifico YOKOHAMA, Kanagawa, Japan)

PEM36-08 Room:312 Time:April 28 11:00-11:15

Study on generation and sustaining mechanism for an SSL during a night of high auroral activity above Tromsoe

TAKAHASHI, Toru[1*] ; NOZAWA, Satonori[1] ; TSUDA, Takuo[2] ; OYAMA, Shin-ichiro[1] ; FUJIWARA, Hitoshi[3] ; TSUTSUMI, Masaki[2] ; KAWAHARA, Takuya[4] ; SAITO, Norihito[5] ; WADA, Satoshi[5] ; KAWABATA, Tetsuya[1] ; MATUURA, Nobuo[1] ; HALL, Chris[6]

[1]STEL, Nagoya Univ., [2]NIPR, [3]Faculty of Science and Technology, Seikei Univ., [4]Faculty of Engineering, Shinshu Univ., [5]RIKEN, [6]Univ. of Tromso

We will report observational results about an SSL (Sporadic Sodium Layer) that appeared on 22 January 2012 above Tromso, Norway (69.6deg N, 19.2deg E). An SSL is sudden formation (more precisely, from observer's viewpoint) of a dense thin sodium layer superposed on a normal sodium layer. Characteristic of an SSL is suitable for investigating, in particular, fine structures in the atmosphere such as small scale waves and turbulences. For example, Tsuda et al., GRL, 2011GL048685 [2011] found out a short-period wavelike structure on an SSL with sodium lidar operated Tromso, Norway.

Some generation mechanisms for SSLs have been proposed and discussed. A high correlation between an SSL and a sporadic E (Es) layer occurrences has been reported, and several authors proposed mechanisms how SSLs are generated by association of the Es layers [e.g., von Zahn and Hansen, JATP, 50, 93-104, 1988]. Kirkwood and von Zahn, JAP, 53, 389-407 [1991] have suggested that a strong electric field that generates an Es layer plays an important role for generation of an SSL as well in the auroral region. Recently, Matuura et al. JGR, 118, 1-12, jgra.50414 [2013] have proposed another mechanism that an electric current loop plays an important role for the convergence of positive ions including metallic ions.

Altitudinal temperature gradients have been also discussed as a candidate for an SSL generation. Clemesha et al., JASTP, j.jastp.2010.03.017 [2010] showed that an SSL tended to be located in the region where the temperature gradient is negative. A sodium lidar measurement exhibited a 40 K temperature increase on the topside of the SSL [Gardner et al., JGR, 98, 16,865-16,873, 1993].

We like to point out two concerns to be improved for the previous studies. First, although an SSL is complex phenomenon resulting from the confluence of various mechanisms, most studies focused on one mechanism alone. Second is a temporal resolution to calculate the neural temperature and sodium density. Since the sodium density inside an SSL varies largely and quickly in an order of seconds, data with insufficient resolution mislead our understanding. The temporal resolutions of five minutes used in previous studies are insufficient. In this study, we have derived neutral temperature and sodium density with a 15 second. Furthermore, we have used data obtained with the EISCAT UHF radar, meteor radar and photometer together with the sodium LIDAR at Tromso.

On 22 January 2012, an SSL was observed by the sodium lidar at about 94 km about 19 minutes after hard auroral precipitations. From 2118 UT to 2142 UT, the sodium density inside the SSL was from 2 and 6 times greater than the background sodium density. After 2142 UT the peak of the SSL went up to 96 km and the SSL became thinner than it was. The peak sodium density decreased, but it was still a few times higher than the background sodium density from 2142 UT to 2400 UT. We have calculated the temperature with a 15 second resolution, and have found that there are no remarkable enhancements in temperature profiles inside the SSL from 2118 to 2142 UT. It would be worth to point out that from 2200 to 2400 UT the SSL stayed in the local temperature minimum of the background atmosphere. Gardner et al. JGR. 2004JD005670 [2005] argued that the sodium density has a negative correlation with temperature at topside of the sodium layer. Therefore, our result is likely to indicate that the temperature profile contributes sustention of the SSL in this event. To investigate other candidate mechanisms for the SSL generation, we have analyzed the EISCAT radar data. The EISCAT radar detected an Es layer simultaneously with the SSL. The Es layer was located on about 94 km altitude where the SSL was located from 2118 UT to 2200 UT. However, after 2200 UT the Es layer was located on 2 km below the SSL. This result is likely to indicate that the Es layer contributes the SSL generation.

Keywords: Sporadic sodium layer, sodium lidar, aurora, EISCAT radar, meteor radar

Japan Geoscience Union Meeting 2014
(28 April - 02 May 2014 at Pacifico YOKOHAMA, Kanagawa, Japan)

PEM36-09 Room:312 Time:April 28 11:15-11:30

Seasonal variation of Polar Mesosphere Winter Echo (PMWE) observed by PANSY radar

NISHIYAMA, Takanori[1*] ; SATO, Kaoru[2] ; TSUTSUMI, Masaki[1] ; SATO, Toru[3] ; NAKAMURA, Takuji[1] ; NISHIMURA, Koji[1] ; KOHMA, Masashi[2] ; TOMIKAWA, Yoshihiro[1] ; EJIRI, Mitsumu[1] ; TSUDA, Takuo[1]

[1]National Institute of Polar Research, [2]Department of Earth and Planet Science, Graduate School of Science, The University of Tokyo, [3]Graduate School of Informatics, Kyoto University

In the lower thermosphere at the altitude of around 100 km, both neutral turbulence and ionization of atmosphere due to solar radiations cause irregularities of reflective index, and as a result back scatter echoes from that altitude are frequently observed by radars on the ground. In the mesosphere, Polar Mesosphere Summer Echo (PMSE) is reported to be a strong echo associated with ice particles, which are produced around the coldest mesopause region in the polar summer, by a number of past radar observations [*Cho and Rottger*, 1997; *Rapp and Lūbken*, 2004]. It should be also noted that occurrence rate of PMSE is very high (80-90%) [*Bremer et al*., 2003]. On the other hand, Polar Mesosphere Winter Echo (PMWE) is also known as back scatter echo from 55 to 85 km in the mesosphere, and it has been observed by MST and IS radar in polar region during winter [e.g., *Ecklund and Balsley*, 1981; *Czechowsky et al*., 1989; *Lūbken et al*., 2006; *Strelnikova and Rapp*, 2013]. Due to the lack of of free electrons and ice particles in the dark and warm mesosphere during winter, it is suggested that PMWE requires strong ionization of neutral atmosphere associated with precipitations of Solar Energetic Particles (SEPs) during geomagnetically disturbed periods [*Kirkwood et al*., 2002; *Zeller et al*., 2006]. However, the detailed generation process of PMWE has not been identified yet, partly because the reported PMWE occurrence rate was quite low (2.9%) [*Zeller et al*., 2006].

In the Ⅷ-th six-year project of the Japanese Antarctic Research Expedition (JARE) from 2010, the middle and upper atmosphere research is one of the sub-projects of the prioritized research project entitled 'Global warming revealed from the Antarctic', and comprehensive ground based observations with various remote sensing instruments for the middle and upper atmosphere have been operating continuously in Syowa station. We analyzed data obtained by PANSY (Program of the Antarctic Syowa MST/IS) radar, which is the core instrument of the project, focusing on PMWE in the context of neutral-plasma atmospheric coupling process between the middle and upper atmosphere. PANSY radar is a 47 MHz VHF radar with 125 kW (full system 500 kW) output power, and it is the largest MST radar composed 5,000 m^2 (full system 20,000 m^2) antenna array in Antarctica at the moment. PANSY has already identified a number of PMWE near local noon since operation of mesosphere observation mode was started in June 2012.

We would like to show seasonal variations of occurrence characteristics of PMWE between June 2012 and July 2013. Taking full advantage of PANSY radar's detectability, we calculated monthly-averaged height-time section of backscatter echo power in austral winter between 2012 and 2013. The result demonstrated that durations of PMWE strongly depended on hours of sunlight, although occurrence heights of PMWE, which range from 60 to 80 km, were fixed on every month and year. These statistical characteristics of PMWE were consistent with previous studies suggesting ionization at the PMWE height due to solar radiation play a dominant role in generation of PMWE [*Zeller et al*., 2006; *Lūbken et al*., 2006]. However, the mean occurrence rate of PMWE estimated by our study was 20-30%, which was considerably higher than that of previous studies. It implies that atmospheric turbulence in the mesosphere would be driven by breakings of atmospheric gravity waves more frequently than past observations, especially in Antarctica, and the role of atmospheric gravity waves cannot be ignored when considering the long-termed climate changes.

Keywords: Polar Mesosphere Winter Echo, PANSY radar, Atmospheric gravity wave, Neutral-plasma interaction

Japan Geoscience Union Meeting 2014
(28 April - 02 May 2014 at Pacifico YOKOHAMA, Kanagawa, Japan)

PEM36-10 Room:312 Time:April 28 11:30-11:45

Analysis of atmospheric gravity waves observed by airglow imaging at Syowa Station (69S,39E), Antarctica

MATSUDA, Takashi S.[1*] ; NAKAMURA, Takuji[2] ; EJIRI, Mitsumu K.[2] ; TSUTSUMI, Masaki[2] ; SHIOKAWA, Kazuo[3] ; TAGUCHI, Makoto[4] ; SUZUKI, Hidehiko[4]

[1]Graduate University for Advanced Studies, [2]National Institute of Polar Research, [3]Solar-Terrestrial Environment Laboratory, Nagoya University, [4]Rikkyo University

Atmospheric gravity waves (AGWs), which are generated in the lower atmosphere, transport significant amount of energy and momentum into the mesosphere and lower thermosphere and cause the mean wind accelerations in the mesosphere. This momentum deposit drives the general circulation and affects the temperature structure. Among many parameters to characterize AGWs, horizontal phase velocity is very important to discuss the vertical propagation. Airglow imaging is a useful technique for investigating the horizontal structures of AGWs at around 90 km altitude. Recently, there are many reports about statistical characteristics of AGWs observed by airglow imaging. However, it is difficult to compare these results obtained at various locations because each research group uses its own method for extracting and analyzing AGW events. In order to deal with huge amounts of imaging data obtained on different years and at various observation sites, without bias caused by different event extraction criteria for the observer, we have developed a new statistical analysis method for obtaining the power spectrum in the horizontal phase velocity domain from airglow image data. This method was applied to the data obtained at Syowa Station, Antarctica, in 2011 and compared with a conventional event analysis in which the phase fronts were traced manually in order to estimate horizontal characteristics. This comparison shows that our new method is suitable for deriving the horizontal phase velocity characteristics of AGWs observed by airglow imaging technique.

We plan to apply this method to airglow imaging data observed at Syowa Station in 2002 and between 2008 and 2013, and also to the data observed at other stations in Antarctica (e.g. Rothera Station (67S, 68W) and Halley Station (75S, 26W)), in order to investigate the behavior of AGWs propagation direction and source distribution in the MLT region over Antarctica. In this presentation, we will report interim analysis result of the data at Syowa Station.

Keywords: atmospheric gravity wave, airglow imaging

Japan Geoscience Union Meeting 2014
(28 April - 02 May 2014 at Pacifico YOKOHAMA, Kanagawa, Japan)

PEM36-11 Room:312 Time:April 28 11:45-12:00

First detection of daytime tweek atmospherics observed at Moshiri and Kagoshima, Japan

OHYA, Hiroyo[1*] ; SHIOKAWA, Kazuo[2] ; MIYOSHI, Yoshizumi[2]

[1]Graduate School of Engineering, Chiba University, [2]Solar-Terrestrial Environment Laboratory, Nagoya University

It is well known that tweek atmospherics can be observed only at night except for solar eclipse days, because daytime attenuation rate of the tweeks is much larger (˜70 dB/1000 km) than that in nighttime (˜3 dB/1000 km). In this presentation, we firstly report detection of daytime tweeks at Moshiri (Geographic coordinate: 44.37^{o}N, 142.27^{o}E) and Kagoshima (31.48^{o}N, 130.72^{o}E), Japan, on non-solar eclipse days in December, 1980. The daytime tweeks were observed both before and during a large magnetic storm during 16-20 December, 1980. The minimum Dst value was -240 nT at 04:00 UT on 20 December. The average occurrence numbers of the daytime tweeks at Moshiri and Kagoshima were 2.7 and 0.3 tweeks per minute, respectively. The local times (LT) when the daytime tweeks occurred were through 07:00 - 17:00 LT at Moshiri, while they were 07:00 - 09:00 LT and 15:00 - 17:00 LT at Kagoshima. All the daytime tweeks show clear frequency dispersion. The average duration was 18.94 ms, while that of nighttime tweeks is ˜50 ms. The average reflection heights of daytime tweeks at Moshiri and Kagoshima were 86.2 km and 94.7 km, respectively. The average reflection heights of nighttime tweeks at Moshiri and Kagoshima in same period were 87.1 km and 92.1 km, respectively. The variation of the daytime tweek reflection height was higher than that of nighttime tweeks. The horizontal propagation distance in daytime cannot be estimated from the dispersion, because the duration was too short to estimate the distance.

We found through a theoretical consideration that the VLF/ELF attenuation on the D-region ionosphere depends not only on the ionospheric height, but also the sharpness of electron density profiles, β. The β is a conventional parameter proposed by Wait and Spies [1964]. When the β increases, the attenuation decreases. Even daytime, when the β is occasionally large, the attenuation would become less down to be able to observe the tweeks. In this talk, we will show the results of the daytime tweeks and discuss their occurrence mechanism.

Japan Geoscience Union Meeting 2014
(28 April - 02 May 2014 at Pacifico YOKOHAMA, Kanagawa, Japan)

PEM36-12 Room:312 Time:April 28 12:00-12:15

Long term variation of geomagnetic Sq field over 100 years

TAKEDA, Masahiko[1*]

[1]Data Analysis Center for Geomag. and Space Magnetism, Kyoto Univ

The long-term variation of the geomagnetic Sq field over 100 years at several observatories was studied in the Y-component as well as the ionospheric conductivity estimated by the IRI model. The amplitude of the geomagnetic Y-component (Sq(Y)) depended strongly on solar activity, and showed features similar to those in the solar activity even when 11-years running averages were employed. The solar activity dependence of Sq(Y) can be fully explained by that of the ionospheric electrical conductivity, and wind velocity tends to be large for low solar activity; and slower in the middle of the 1900s in response to higher long-term solar activity. On the other hand, other long-term variations were not clear in the wind velocity. Although the dynamo theory predicts that the Sq current is enhanced when geomagnetic main field intensity decreases, the result of the present analysis does not necessarily support this prediction.

Keywords: geomagnetic daily variation, long-term variation, solar activity, main field strength, elecric conductivity, wind velocity

Japan Geoscience Union Meeting 2014
(28 April - 02 May 2014 at Pacifico YOKOHAMA, Kanagawa, Japan)

PEM36-13 Room:312 Time:April 28 12:15-12:30

Long-term variation in the upper atmosphere as seen in the geomagnetic solar quiet (Sq) daily variation

SHINBORI, Atsuki[1*] ; KOYAMA, Yukinobu[2] ; NOSE, Masahito[2] ; HORI, Tomoaki[3] ; OTSUKA, Yuichi[4] ; YATAGAI, Akiyo[4]

[1]Research Institute for Sustainable Humanosphere (RISH), Kyoto University, [2]Data Analysis Center for Geomagnetism and Space Magnetism Graduate School of Science, Kyoto Universi, [3]Nagoya University Solar Terrestrial Environment Laboratory Geospace Research Center, [4]Solar-Terrestrial Environment Laboratory, Nagoya University

It has been well-known that the geomagnetic field on the ground shows a regular variation with a fundamental period of 24 hours during a solar quiet day. This daily variation depends on local time, latitude, season and solar cycle and has been called solar quiet (Sq) geomagnetic field daily variation. The Sq variation is mainly produced by magnetic effects due to ionospheric currents flowing in the E region of the ionosphere around 105 km. The global pattern of the Sq variation of the H-component shows positive and negative changes in the equatorial and middle-latitude regions around noon, respectively. The Sq current system expected from the geomagnetic field perturbations consists of two large current vortices: one is an anticlockwise current in the northern hemisphere and the other is a clockwise current in the southern hemisphere. The Sq current is dominant in the daytime ionosphere where ionospheric conductivity is relatively large, and is driven by electric fields originating from the ionospheric dynamo via the interaction between ionized and neutral particles. According to the Ohm's law, the main variables in the Sq amplitude are the ionospheric conductivity, the polarization electric field, the solar diurnal tide, and the intensity of the ambient magnetic field at the E-region height. Then, to investigate the long-term variation in the Sq amplitude is important for understanding the physical mechanism of long-term variation in the upper atmosphere related to solar activity and lower atmospheric change such as global warming. In this study, we investigated long-term variation in the Sq amplitude using 1-hour geomagnetic field data obtained from 184 geomagnetic observation stations within a period of 1947-2012 in order to clarify the physical mechanism of long-term variation in the upper atmosphere. For the analysis of long-term observation data obtained from a lot of geomagnetic stations, we took advantage of the IUGONET data analysis system (metadata database search system and data analysis software). The Sq amplitude is defined as a difference of the H-component of geomagnetic field between the maximum and minimum values each solar quiet day. We identified the solar quiet day as the day when the maximum Kp value is less than 4 for each day. As a result, the Sq amplitude observed at all the geomagnetic stations showed a clear dependence on the 11-year solar activity and it tended to be enhanced significantly during solar maximum. The Sq amplitude became the smallest around the minimum of 23/24 solar cycle in 2008-2009. The relationship between the Sq amplitude and F10.7 solar activity index was not linear but nonlinear. This nonlinearity could be interpreted as the decrease of production rate of electrons and ions in the ionosphere for the strong extreme ultraviolet (EUV) and ultraviolet (UV) fluxes. In order to minimize an effect of solar activity including the long-term variation in the Sq amplitude, we calculated second orders of fitting curve between the F10.7 solar index and Sq amplitude during 1947-2012, and examined the residual Sq amplitude defined as the deviation from the fitting curve. As a result, majority of the residual Sq trends passed through the trend test showed a negative value without dependence on geographical latitude and longitude. The tendency was strong in India, the southern part of Africa, and the northern part of America and Europe. In a region of northern part of America and Europe, the secular variation of magnetic inclination becomes relatively large, compared with other regions. Therefore, the long-term trend in the residual Sq amplitude could be linked to a change in the ionospheric conductivities associated with the secular variation of the ambient magnetic field and the upper atmosphere and electro motive force (UxB) via the interaction between ionized and neutral particles.

Keywords: Geomagnetic solar quiet daily variation, Solar activity, Long-term variation, Geomagnetic secular variation, Ionospheric conductivity, Global warming

Japan Geoscience Union Meeting 2014
(28 April - 02 May 2014 at Pacifico YOKOHAMA, Kanagawa, Japan)

PEM36-14 Room:312 Time:April 28 12:30-12:45

Temporal increases of horizontal speed of frontal Es observed by HFD

TOMIZAWA, Ichiro[1*] ; MIYAWAKI, Masami[1]

[1]Center for Space Science and Radio Engineering, The University of Electro-Commnunications

In the yearly analysis of the horizontal speed of frontal Es by using the HFD observation data of the year 2012, we found some events which showed temporal increase and then decrease within the time scale from 40 to 270 minutes. The rate of the temporal speed enhancements were only 2.4 % in all frontal Es events in 2012, and the enhances were mainly observed aroun 21h JST in summer. The rate of the speed enhancement were less than 30 %, but some peak speeds increased up to more than 200 m/s. The duration times varied from 40 to 300 min, but most of the events terminated within 150 min. The average leading and trailing times were 35 and 50 min, respectively, so the trailing part took long time. The cause of temporal speed variation can be related to time variation of horizontal electric field or of horizontal wind speed of neutral atmosphere in the E layer. The former should show coincidence over the wide area but the latter would show some time difference. Analyzing pair data over 100 km separation, we obtained time delay less than 20 min. It is therefore interpreted that the temporal speed increase is caused by the change of the horizontal wind speed. Because the distance between successive Es front shows the minimum of less than 50 km around the speed peak, and increases upto 200 km both to the start and to the end, it can be attributed to the inequally spaced Es front. Combining all separation distances for each event, we get the outer size of the temporal variation as 400 km for 65 %, and as the maximum of 1400 km. On the otherhand, it can be related to a non-isotropic structure because the peak speed did show different values for the separate stations. Based on those observational results, it is concluded that the temporal speed increase may be introdued by a spiral-like, instead of linear, structure.

Keywords: frontal Es, horizontal speed, temporal increase, HF Doppler observation

Japan Geoscience Union Meeting 2014
(28 April - 02 May 2014 at Pacifico YOKOHAMA, Kanagawa, Japan)

PEM36-15 Room:312 Time:April 28 14:15-14:30

Study of medium-scale traveling ionospheric disturbances (MSTID) with sounding rockets and ground observations

YAMAMOTO, Mamoru[1*] ; KATO, Tomohiro[1] ; ISHISAKA, Keigo[2] ; YOKOYAMA, Tatsuhiro[3] ; IWAGAMI, Naomoto[3] ; TAKAHASHI, Takao[5] ; TANAKA, Makoto[5] ; ENDO, Ken[6] ; KUMAMOTO, Atsushi[6] ; WATANABE, Shigeto[7] ; YAMAMOTO, Masa-yuki[8] ; ABE, Takumi[9] ; SAITO, Susumu[10] ; TSUGAWA, Takuya[3] ; NISHIOKA, Michi[3] ; BERNHARDT, Paul[11] ; LARSEN, Miguel[12]

[1]RISH, Kyoto University, [2]Toyama Prefectural University, [3]NICT, [4]School of Science, University of Tokyo, [5]ICT Education Center, Tokai University, [6]School of Science, Tohoku University, [7]School of Science, Hokkaido University, [8]Kochi University of Technology, [9]JAXA/ISAS, [10]ENRI, [11]NRL, [12]Clemson University

Medium-scale traveling ionospheric disturbance (MSTID) is an interesting phenomenon in the F-region. The MSTID is frequent in summer nighttime over Japan, showing wave structures with wavelengths of 100-200 km, periodicity of about 1 hour, and propagation toward the southwest. The phenomena are observed by the total electron content (TEC) from GEONET, Japanese dense network of GPS receivers, and 630 nm airglow imagers as horizontal pattern. It was also measured as Spread-F events of ionograms or as field-aligned echoes of the MU radar. MSTID was, in the past, explained by Perkins instability (Perkins, 1973) while its low growth rate was a problem. Recently 3D simulation study by Yokoyama et al (2009) hypothesized a generation mechanism of the MSTID, which stands on electromagnetic E/F-region coupling of the ionosphere. The hypothesis is that the MSTID first grows with polarization electric fields from sporadic-E, then show spatial structures resembling to the Perkins instability. We recently conducted a observation campaign to check this hypothesis. We launched JASA ISAS sounding rockets S-310-42 and S-520-27 at 23:00 JST and 23:57JST on July 20, 2013 while an MSTID event was monitored in real-time by the GPS-TEC from GEONET. We found 1-5mV/m northeastward/eastward electric fields during the flight. Variation of electric fileds were associated with horizontal distribution of plasma density. Wind velocity was measured by the TME and Lithium releases from S-310-42 and S-520-27 rockets, respectively, showing southward wind near the sporadic-E layer heights. These results are consistent to the expected generation mechanism shown above. In the presentation we will discuss electric-field results and its relationship with plasma density variability together with preliminary results from the neutral-wind observations.

Keywords: MSTID, Sounding rocket, Electric field, GPS-TEC, Observation campaign

Japan Geoscience Union Meeting 2014
(28 April - 02 May 2014 at Pacifico YOKOHAMA, Kanagawa, Japan)

PEM36-16 Room:312 Time:April 28 14:30-14:45

Characteristics of O630nm emission associated with equatorial ionization anomaly obtained with IMAP/VISI

SAKAMOTO, Daiki[1] ; SAKANOI, Takeshi[1*] ; PERWITASARI, Septi[1] ; OTSUKA, Yuichi[2] ; SAITO, Akinori[3] ; AKIYA, Yusuke[3] ; HOZUMI, Yuta[3] ; YAMAZAKI, Atsushi[4]

[1]Grad. School of Science, Tohoku University, [2]STEL, Nagoya University, [3]Grad. School of Science, Kyoto University, [4]ISAS / JAXA

The Equatorial Ionization Anomaly (EIA) is occurred by plasma upwelling due to eastward electric field in the dayside magnetic equator, and descends to both northern and southern hemispheres along the field line. Density maximum appears around geomagnetic latitudes of +/-15 degree at both hemispheres. Since most of the past studies carried out with ground experiments, it is difficult to observe a wide area and study the variability of the northern and southern O630nm emission associated with EIA.

IMAP/VISI on the International Space Station(ISS) measures O630 nm airglow emission in the nightside hemisphere at an altitude of 400km. It covers the latitudinal range between +/-52 degrees with a typical spatial resolution of 1x14 km. Because of the wide observation coverage, it is possible to observe the variability of O630nm airglow associated with the EIA.

In this study, we carried out a statistical analysis using IMAP/VISI data from September 2012 to December 2013 to understand the variability of O630nm airglow associated with the EIA, particularly on its local time dependence, seasonal variation and geomagnetic activity. We derived the integrated intensity of O630nm emission along latitude with the four criteria as follows: (1) The O630nm emission in the EIA is greater than the background airglow that was determined by emission intensity in the middle latitude. (2) Latitudinal distribution of O630nm emission in the EIA is fully measured. (3) The northern and southern O630nm emission in the EIA is clearly separated. (4) The moon phase is smaller than 0.5. In case that the moon phase is bigger than 0.5 then we used the data when the moon did not appear.

We find that the time dependence of O630nm emission which is decreased from the evening toward the post mid-night. But there is a large variance in the intensity at the same local time. This fact suggests that other process, such as the longitude and/or seasonal variation, may affect the O630nm emission associated with the EIA in addition to the local time dependence.

On the seasonal dependence, we find that O630nm emission in the EIA in the winter hemisphere is greater than that in the summer hemisphere. This is consistent with the model that the thermospheric tidal wind affects the 630 nm intensity, namely, the tidal wind decreases the altitude of O630 nm emission layer and finally gain the O630 nm intensity.

To examine the longitudinal dependence, we used the data in equinox (September and October, 2013) and find that O630nm emission in the EIA in the northern hemisphere is greater than that in the southern hemisphere where the dip equator is the south of geographic equator (longitude is between 200 degree ? 310 degree). This is also consistent with the model that the thermospheric tidal wind controls the O630 nm intensity by making a vertical motion of emission layer.

Finally, we investigate the magnetic storm dependence on O630 nm intensity and find that significant decrease of O630nm intensity in the EIA happens during the period when the Dst index is larger than 90. From this fact, it is plausible that westward electric field in Region 2 current system penetrates to the low latitude region during the main phase of magnetic storm and reduce the formation of EIA.

Keywords: ISS, airglow, thermosphere, ionosphere, equatorial ionization anomarly, IMAP

Japan Geoscience Union Meeting 2014
(28 April - 02 May 2014 at Pacifico YOKOHAMA, Kanagawa, Japan)

PEM36-17 Room:312 Time:April 28 14:45-15:00

Analysis of the airglow structures using the simultaneous observations by ISS-IMAP and all-sky imagers

YUKINO, Hideko[1*] ; SAITO, Akinori[1] ; OTSUKA, Yuichi[2] ; SAKANOI, Takeshi[3]

[1]Dept. of Geophysics, Kyoto Univ., [2]STEL, Nagoya Univ., [3]Grad. School of Science, Tohoku Univ.

The spatial structure of the atmospheric gravity waves in the mesosphere was analyzed using the simultaneous observational data of ISS-IMAP and the all-sky imager at Hawaii. There are a plenty of ground-based observations of the atmospheric gravity waves in the mesosphere and the thermosphere. The problem of the ground-based observation is that it cannot distinguish spatial variations from temporal variations for the structures whose scale size is larger than its field-of-view. ISS-IMAP was launched on July 21, 2012 to observe the atmospheric gravity waves whose scale size is larger than 100 km. The altitude of the International Space Station (ISS) flies around 400 km altitude, and its orbital inclination angle is 51.6 degrees. ISS-IMAP/VISI (Visible-light and infrared Spectrum Imager) observes the airglow in the mesosphere and the ionosphere. The spatial resolution of the VISI imaging observation is from 10 km to 25 km. The airglow wavelengths observed by VISI are 630 nm, 730 nm, and 762 nm and by the ground-based all-sky image of Hawaii (20.48 N, 156.2 W) are 630 nm and 557.7-nm with 5.5 minutes interval. The observational data of ISS-IMAP/VISI and an all-sky imager in Hawaii were investigated for the nights when VISI made the observation over Hawaii, and the sky over the imager was clear. The night when the plasma bubble was detected by the ground-based all-sky imager, the plasma bubble was detected by the 630nm airglow observation of ISS-IMAP/VISI. The spatial and vertical structures of the airglow that were observed by the ground-based imager and the ISS-IMAP/VISI were analyzed. The sensitivity of the observation of ISS-IMAP/VISI will also be discussed in the comparison of the ground-based observation.

Keywords: airglow, plasma bubble, ISS-IMAP

Japan Geoscience Union Meeting 2014
(28 April - 02 May 2014 at Pacifico YOKOHAMA, Kanagawa, Japan)

PEM36-18 Room:312 Time:April 28 15:00-15:15

Horizontal structures of ionized Helium in the topside ionosphere of dusk side observed by ISS-IMAP/EUVI

HOZUMI, Yuta[1*] ; SAITO, Akinori[1] ; YAMAZAKI, Atsushi[2] ; MURAKAMI, Go[2] ; YOSHIKAWA, Ichiro[3]

[1]Department of Geophysics, Graduate School of Science, Kyoto University, [2]Institute of Space and Astronautical Science / Japan Aerospace Exploration Agency, [3]The University of Tokyo

Horizontal structures of ionized Helium in the topside ionosphere of dusk side were obtained with the Extreme Ultra Violet Imager (EUVI) of the ISS-IMAP (Ionosphere, Mesosphere, upper Atmosphere and Plasmasphere mapping) mission. EUVI has taken image of He He II radiation (30.4 nm) from the International Space Station (ISS) since October 2012. In this work, images taken in 2013 were analyzed. North-south asymmetry and longitudinal structure of ionized Helium were found. Seasonal dependence of these horizontal structures will be discussed.

Keywords: Topside ionosphere, ISS-IMAP, Ionoized Helium

Japan Geoscience Union Meeting 2014
(28 April - 02 May 2014 at Pacifico YOKOHAMA, Kanagawa, Japan)

PEM36-19 Room:312 Time:April 28 15:15-15:30

Study of ionospheric disturbance characteristics during solar flare events using the SuperDARN Hokkaido radar

WATANABE, Daiki[1] ; NISHITANI, Nozomu[1*]

[1]Solar-Terrestrial Environment Laboratory, Nagoya University

Ionospheric disturbances during solar flare events have been studied by various kinds of observation instrument in the last few decades. Kikuchi et al. (1985) reported on the positive Doppler shift in the HF Doppler system data during solar flare events, and indicated that there are two possible factors of Doppler shift, i.e., (1) apparent ray path decrease by changing refraction index due to increasing electron densities in the D-region ionosphere, and (2) ray path decrease due to descending reflection point associated with increasing electron density in the F-region ionosphere.

In this study, we use the SuperDARN Hokkaido Radar to investigate the detailed characteristics of solar flare effects on ionospheric disturbances. We focus on the positive Doppler shift of ground / sea scatter echoes just before sudden fade-out of echoes. Davies et al. (1962) showed that if the factor (1) is dominant, the Doppler shift should have positive correlation with slant range and negative correlation with elevation angle and frequency. On the other hand, if the factor (2) is dominant, the Doppler shift should have negative correlation with slant range and positive correlation with elevation angle and frequency. While Kikuchi et al. (1985) studied solar flare events and mainly discussed frequency dependence of Doppler shift, we study mainly slant range and elevation angle dependence, for the first time to the best of our knowledge. We found that the factor (1), in other words, increase of electron densities at D-region ionosphere, is dominant during solar flare events. This result is consistent with that of Kikuchi et al. (1985). In order to study characteristics of ionospheric disturbance in more detail, we are studying relationship between timing / amplitude of ionospheric disturbance and that of the solar irradiation changes, by comparing the HF radar data with high wavelength resolution irradiation data for X-ray and EUV from RHESSI and SDO satellites. Generally, X-ray radiation becomes more important for the changes in the D-region during solar flare events. Therefore we investigate relationship between X-ray flux changes and electron density variation in the D-region ionosphere intensively. Furthermore, we estimated electron density changes in the ionsosphere by analyzing elevation angle dependence of Doppler shift in radar echoes quantitatively. We are estimating electron density by considering chemical reaction and photoreaction caused by solar radiation. We will compare the two electron density changes deduced from different two ways and evaluate the amplitude of ionospheric disturbance observed by the HF radar. More detailed analysis result will be reported.

Keywords: SuperDARN, Hokkaido radar, solar flares, ionospheric disturbances, photochemical reaction, range dependence

Japan Geoscience Union Meeting 2014
(28 April - 02 May 2014 at Pacifico YOKOHAMA, Kanagawa, Japan)

PEM36-20 Room:312 Time:April 28 15:30-15:45

Thermospheric tidal effects on the ionospheric midlatitude summer nighttime anomaly

CHEN, Chia-hung[1*] ; LIN, Charles[1] ; CHANG, Loren[2] ; HUBA, J. D.[3] ; SAITO, Akinori[4] ; LIU, Jann-yenq[2]

[1]Department of Earth Science, National Cheng Kung University, Tainan, Taiwan, [2]Institute of Space Science, National Central University, Chung-Li, Taiwan, [3]Plasma Physics Division, Naval Research Laboratory, Washington, D. C., USA, [4]Department of Geophysics, Kyoto University, Kyoto, Japan

This study use a 3D physics-based ionospheric model, SAMI3, coupled with the National Center for Atmospheric Research Thermosphere Ionosphere Electrodynamics General Circulation Model (TIEGCM) and Global Scale Wave Model (GSWM) to simulate the mesospheric and lower thermosphreic tidal effects on the development of midlatitude summer nighttime anomaly (MSNA). Using this coupled model, the diurnal variation of MSNA electron densities at 300 km altitude is simulated on both June solstice (day of year (DOY) 167) and December solstice (DOY 350) in 2007. Simulation results show successful reproduction of the southern hemisphere MSNA structure including the eastward drift feature of the southern MSNA, which is not reproduced by the default SAMI3 runs using the neutral winds provided by the empirical Horizontal Wind Model 93 (HWM93) neutral wind model. A linear least squares algorithm for extracting tidal components is utilized to examine the major tidal component affecting the variation of southern MSNA. Results show that the standing diurnal oscillation component dominates the vertical neutral wind manifesting as a diurnal eastward wave-1 drift of the southern MSNA in the local time frame. We also find that the stationary planetary wave-1 component of vertical neutral wind can cause diurnal variation of the summer nighttime electron density enhancement around the midlatitude ionosphere.

Keywords: Midlatitude Summer Nighttime Anomaly, thermospheric tidal effect

Japan Geoscience Union Meeting 2014
(28 April - 02 May 2014 at Pacifico YOKOHAMA, Kanagawa, Japan)

PEM36-21 Room:312 Time:April 28 15:45-16:00

Horizontal ion drag effect on the thermospheric mass density anomaly in the cusp

MATSUMURA, Mitsuru[1*] ; TAGUCHI, Satoshi[2]

[1]Center for Space Science and Radio Engineering, University of Electro-Communications, [2]Graduate School of Informatics and Engineering, University of Electro-Communications

CHAMP satellite observations have revealed that the thermospheric mass density in the cusp region is statistically larger by a factor of about 1.3 than that in its adjacent region. Many studies have pointed out that the upward mass transport due to heating is important for the generation of the mass density anomaly, but what confines the heating rate to the cusp is controversial. We have paid attention to the effect of the horizontal mass transport. Our reasoning on this point is as follows. Ionospheric convection gives momentum to the neutral air through ion drag, and the ion drag can modify the distribution of the neutral mass density. Our recent results from numerical simulations have indicated that the ion drag enhances the neutral mass density in the cusp that the terminator overlaps. In this paper, we report on the result about more general situations including cases when the terminator is located away from the cusp. Our results show that the mass density anomaly is confined to the cusp by ion drag, irrespective of the location of the terminator. We show detailed relations between the ion drag distribution and the mass density enhancement or depletion.

Keywords: thermosphere, mass density, cusp, CHAMP satellite

Japan Geoscience Union Meeting 2014
(28 April - 02 May 2014 at Pacifico YOKOHAMA, Kanagawa, Japan)

PEM36-22 Room:312 Time:April 28 16:15-16:30

Edge of polar cap patches

HOSOKAWA, Keisuke[1*] ; TAGUCHI, Satoshi[1] ; OGAWA, Yasunobu[2]

[1]University of Electro-Communications, [2]National Institute of Polar Research

A highly sensitive all-sky EMCCD airglow imager (ASI) has been operative in Longyearbyen, Norway (78.1N, 15.5E) since October 2011. One of the primary targets of this optical observation is a polar cap patch which is defined as an island of enhanced plasma density in the F region drifting anti-sunward across the central polar cap. Since the electron density within patches is often increased by a factor of 2?10 above that in the surrounding region, all-sky airglow measurements at 630.0 nm wavelength are capable of visualizing their spatial distribution in 2D fashion.

During a 4-h interval on the night of December 4, 2013, a series of polar cap patches was observed by the ASI in Longyearbyen. By using the high-quality ASI images, we estimated the gradients in the leading/trailing edges of the patches and found that the gradient in the leading edge is 2-3 times steeper than that in the trailing edge. We also identified finger-like undulating structures growing along the trailing edge of the patches. Generation of these fingers is probably governed by a structuring through the gradient-drift instability which is known to occur only along one side of patches.

From these observations, we suggest that such a structuring process can transport and mix the patch plasma across their trailing edges so that the scale size of the edges get extended. This means that the structuring through the plasma instability can strongly influence the large-scale shape of patches. Such a knowledge is of particular importance for better understanding the space weather effects of patches on the trans-ionospheric satellite communications in the polar cap region.

Keywords: Polar cap ionosphere, Airglow, Polar patches, Plasma instability

Japan Geoscience Union Meeting 2014
(28 April - 02 May 2014 at Pacifico YOKOHAMA, Kanagawa, Japan)

PEM36-23 Room:312 Time:April 28 16:30-16:45

Correlation analysis between equatorial electrojet,pre-reversal enhancement and equatorial spread F in Southeast Asia

KUNITAKE, Manabu[1*] ; TSUGAWA, Takuya[1] ; YOKOYAMA, Tatsuhiro[1] ; NISHIOKA, Michi[1] ; YAMAMOTO, Kazunori[1] ; ISHIBASHI, Hiromitsu[1] ; NAGATSUMA, Tsutomu[1] ; MARUYAMA, Takashi[1] ; ISHII, Mamoru[1] ; SHIOKAWA, Kazuo[2]

[1]NICT, [2]STE Lab., Nagoya Univ.

At the equatorial latitudes, the reversal of dayside eastward electric field to westward around sunset is often accompanied by a strengthened eastward electric field. The strengthened eastward electric field is called as the pre-reversal enhancement (PRE). PRE is considered to be the primary process acting on the equatorial spread F (ESF) onsets. Relationships between PRE strength, ESF onsets, and equatorial electrojet (EEJ) strength have been investigated by using ionosonde observation and magnetometer observation. Uemoto et al. (2010) found that PRE strength and ESF onsets are suppressed when pre-sunset integrated EEJ from 2 hours to 1 hour prior to sunset is negative owing to the evening counter electrojet, by statistical analysis of observations in the Southeast Asia low-latitude ionospheric network (SEALION). Their analyzing period is from November 2007 to October 2008. The period is in solar minimum phase.

We use SEALION data from 2007 to 2013. Therefore, our analyzing period covers not only solar minimum phase but also solar maximum phase. Statistical analyses for each year are conducted. Further, detailed case study is conducted. Significant day-to-day variations of EEJ strength, PRE strength, and ESF onsets are picked up from these seven years data. Then, we investigate how and to what extent day-to-day variations of EEJ strength relate to the day-to-day variations of PRE strength and ESF onsets. The magnetometer data in our study were obtained at Phuket (geographic lat. 8.09N, geographic long. 98.32E, dip lat. -0.2) and Kototabang (0.20S, 100.32E, dip lat. -10.1). The ionosonde data in our study were obtained at Chumphon (10.72N, 99.37E, dip lat. 3.0), Chiang Mai (18.76N, 98.93E, dip lat. 12.7), and Kototabang (0.20S, 100.32E, dip lat. -10.1).

Reference

Uemoto J., T. Maruyama, S. Saito, M. Ishii, and R. Yoshimura, Relationships between pre-sunset electrojet strength, pre-reversal enhancement and equatorial spread-F onset, Ann. Geophys., vol. 28, pp. 449-454, 2010.

Acknowledgements

The ionosonde at Chiang Mai is operated under agreements between NICT, Japan and Chiang Mai University (CMU), Thailand. The ionosonde at Chumphon and the magnetometer at Phuket are operated under agreements between NICT and King Mongkut ′ s Institute of Technology Ladkrabang (KMITL), Thailand. The magnetometer at Kototabang has been operated in collaboration among the Solar-Terrestrial Environment Laboratory (STEL), Nagoya University, Japan, the Research Institute for Sustainable Humanosphere (RISH), Kyoto University, Japan, and the National Institute of Aeronautics and Space (LAPAN), Indonesia. The ionosonde at Kototabang has been operated in collaboration among NICT, RISH and LAPAN. We thank Mr. Yamazaki for manual scaling of ionosonde data.

Keywords: electrojet, equatorial spread F, day-to-day variation, SEALION

Japan Geoscience Union Meeting 2014
(28 April - 02 May 2014 at Pacifico YOKOHAMA, Kanagawa, Japan)

PEM36-24 Room:312 Time:April 28 16:45-17:00

Low-latitude ionosphere dynamics as deduced from meridional ionosonde chain: Ionospheric ceiling

MARUYAMA, Takashi[1*] ; UEMOTO, Jyunpei[1] ; ISHII, Mamoru[1] ; TSUGAWA, Takuya[1] ; SUPNITHI, Pornchai[2] ; KOMOLMIS, Tharadol[3]

[1]National Institute of Information and Communications Technology, [2]King Mongkut's Institute of Technology Ladkrabang, [3]Chiang Mai University

Peculiar ionospheric features at low latitudes originate in the earth's magnetic field configuration that has a shape of arch. Near the magnetic equator, the daytime eastward electric field raises the ionosphere to high altitudes where the ion-neutral collision frequency reduces. The ionospheric plasma slips down over off-equatorial latitudes along the arch-shaped magnetic field line by the earth's gravity acceleration and the reduced ion-neutral drag, which is called the fountain effect. As a consequence, the latitudinal distribution of ionospheric critical frequency (foF2) forms two crests at low latitudes and a trough above the magnetic equator, which is well-known equatorial anomaly in foF2 distribution. As for the diurnal variation of the ionosphere above the magnetic equator, foF2 once increases in the morning and decreases before noon along with the development of the equatorial anomaly, which is called noon bite-out. Another feature at the magnetic equator, associated with the fountain effect, is the relatively steady ionospheric peak height (hmF2) around noon, even though the EXB drift is upward throughout the daytime. However, not much attention has been paid to hmF2 except for the time rate of change of it in connection with the vertical plasma drift velocity.

Interest in the equatorial anomaly has been focused mostly on foF2 (or NmF2), and there have been a few studies on hmF2 variations associated with equatorial anomaly development. In this paper, we revisit the equatorial anomaly in terms of height variations. For this purpose, we analyzed scaled ionogram parameters from three stations located along the magnetic meridian that is a primary component of Southeast Asia low-latitude ionospheric network (SEALION); one at the magnetic equator and the others at conjugate off-equatorial latitudes near 10 degrees magnetic latitude.

The daytime hmF2 was investigated for each season during the solar minimum period, 2006-2007 and 2009. The peak height increased for approximately 3 hr after sunrise at all locations, as expected from the daytime upward EXB drift. The apparent upward drift ceased before noon at the magnetic equator, while the layer continued to increase at the off-equatorial latitudes, reaching altitudes higher than the equatorial height around noon. The noon time restricted layer height at the magnetic equator did not depend on the season, while the maximum peak height at the off-equatorial latitudes largely varied with season. The daytime specific limiting height of the equatorial ionosphere was termed ionospheric ceiling. Numerical modeling using the SAMI2 code reproduced the features of the ionospheric ceiling quite well. Dynamic parameters provided by the SAMI2 modeling were investigated and it was shown that the ionospheric ceiling is another aspect of the fountain effect, in which increased diffusion of plasma at higher altitudes has a leading role.

Keywords: equatorial anomaly, fountain effect, ionospheric ceiling, EXB drift, SEALION

Japan Geoscience Union Meeting 2014
(28 April - 02 May 2014 at Pacifico YOKOHAMA, Kanagawa, Japan)

PEM36-25 Room:312 Time:April 28 17:00-17:15

Three-dimensional high-resolution plasma bubble modeling

YOKOYAMA, Tatsuhiro[1*] ; SHINAGAWA, Hiroyuki[1] ; JIN, Hidekatsu[1]

[1]National Institute of Information and Communications Technology

Equatorial plasma bubble (EPB) is a well-known phenomenon in the equatorial ionospheric F region. As it causes severe scintillation in the amplitude and phase of radio signals, it is important to understand and forecast the occurrence of EPB from a space weather point of view. The development of EPB is known as a evolution of the generalized Rayleigh-Taylor instability. Numerical modelings of the instability on the equatorial two-dimensional plane have been conducted since the late 1970's, and the nonlinear evolution of the instability has been clearly presented. Recently, three-dimensional (3D) modelings became popular tools for further understanding of the development of EPB such as 3D structure of EPB, meridional wind effects and gravity wave seeding. One of the biggest advantages of the 3D model is that the off-equatorial E region which is coupled with the equatorial F region can be included in the model. It is known from observations that the conductance of the off-equatorial E region controls the growth rate of the Rayleigh-Taylor instability, that is, sudden decrease of the E-region conductance around the sunset accelerates the evolution of the instability. We have developed a new 3D high-resolution model for EPB, and studied internal structure of EPB and the contribution of the off-equatorial E region. As it is necessary to use high-order numerical schemes to capture sharp plasma density gradient of EPB, we adopted the CIP scheme which can keep the third-order accuracy in time and space. The simulated EPB has asymmetrical density gradients at east and west walls, and the growth rate changes significantly depending on the condition of the off-equatorial E region. In the future, we will integrate the high-resolution model into whole atmosphere-ionosphere coupled model (GAIA) to study the growth of EPB under the realistic background conditions.

Keywords: plasma bubble, equatorial spread F, equatorial ionosphere, numerical simulation

Japan Geoscience Union Meeting 2014
(28 April - 02 May 2014 at Pacifico YOKOHAMA, Kanagawa, Japan)

PEM36-P01 Room:Poster Time:April 28 18:15-19:30

Basic development of a small balloon-mounted telemetry with its operation system

KONO, Hiroki[1*] ; KAKINAMI, Yoshihiro[1] ; YAMAMOTO, Masa-yuki[1]

[1]Kochi Univ. of Tech

1. Introduction

In Japan, the high altitude balloon for scientific observation has been continuously launched by JAXA. The balloon has a possibility to reach 50 km altitude without severe environmental condition for onboard equipments, being operated with lower cost than sounding rockets, however, development of such large-scale scientific observating balloons by university laboratories is still difficult. Being coupled with rapid improvement of tiny semiconductor sensors recently, laboratory-basis balloon experiments using small weather balloons have been becoming easily in these years (e.g. Near Space Ventures, Inc., 2013).

Although the balloon is very small as its diameter of 6 feets, excluding its extra buoyancy and the weight of the balloon itself, it is expected that loading mass capacity of about 2 kg is remained for payloads to send it up to about 35 km. However, operation of such small balloons in Japan is not in general because precise prediction of a landing area of the payload is difficult, thus high-risk situation for balloon releases is still remained. In this study, we aim to achieve practical engineering experiments of weather balloons in Japan in order to operate laboratory level scientific observation within a university. Here we report an approach of developing many devices currently in progress.

2. Equipments development

We have been developing devices onboard a small tethered balloon for the future weather balloon release experiments. That is, one is a small-size and light-weight telemeter system of about 250 g that can be mounted on a commercially available balloon, while another is a ground station device that receives data from the telemeter. A combination of a wireless module, a GPS receiver, a barometer, a temperature and humidity meter, a camera, an accelerometer, an electronic compass, a power monitor sensor is mounted on the telemeter, and the measured values by each sensors can be transmitted in real time to the ground station device. Newly developed software for balloon operation can be run on a PC connected with the ground station device, it is possible to provide the operator the sensor information visualized in real time based on the position coordinates set on the ground station device using the software before the launch.

Real-time mapping of the balloon coordinates can be realized to rewrite a KML file to be input into the Google Earth continuously. In addition, azimuth and elevation of the balloon can be calculated by spherical trigonometry from obtained the GPS position. Providing these angles to a newly developed rotater to be mounted on a camera tripod, it is possible to track a small antenna automatically to the balloon direction continuously.

3. Result of the experiment

A tethered balloon experiment was performed for evaluating the developed telemeter system, however, there occurred unexpected issue in the communication distance. As a result, in the telemeter line, operating limit of the distance between the ground station and the telemeter is significantly shortened to approximately 110 m. It was almost different from our pre-experiment confirmation of a packet loss rate of 0% at 270 m distance in a preliminary experiment on ground.

Therefore, evaluation of the antenna rotator was carried out only at close range, i.e., in severe condition. It is because maximum elevation of the rotator was limited physically at 50 degrees or less, and there exists about 5 to 10 m error in the GPS positioning operated in the single receiver mode.

Nevertheless, it was possible to track the balloon continuously in a stable situation even in the shortened communication distance. In addition, the software and telemeter system worked as expected, the problem was not found in particular.

In this presentation, the data obtained by the tethered balloon experiment and detail of the developed equipments will be shown.

Keywords: Weather balloon, Tethered balloon, Stratosphere, Upper atmosphere, Telemeter, Embedded system

Japan Geoscience Union Meeting 2014
(28 April - 02 May 2014 at Pacifico YOKOHAMA, Kanagawa, Japan)

PEM36-P02 Room:Poster Time:April 28 18:15-19:30

Impacts of stratospheric sudden warming events in the mesosphere and lower thermosphere

WATANABE, Kumiko[1*] ; TANAKA, Takashi[1] ; MIYOSHI, Yasunobu[2]

[1]Department of Earth and Planetary Sciences, Graduate School of Sciences, Kyushu University, [2]Department of Earth and Planetary Sciences, Faculty of Sciences, Kyushu University

Impacts of stratospheric sudden warming (SSW) events on the middle and upper atmosphere have been widely recognized. However, due to an insufficient number of global observations, SSW's effects on the general circulation in the mesosphere and lower thermosphere (MLT) are not well known. In this study, we investigate the short term variation of the temperature, zonal wind and meridional wind in the MLT region during SSW events using a general circulation model that contains the region from the troposphere to the thermosphere. We conducted GCM simulation with meteorological reanalysis data during the period from November 1, 2008 to March 31, 2010. Our results show that the temperature drop occurs in the Southern hemisphere, during SSW events. This means that SSW influences the general circulation in the summer hemisphere. Furthermore, it is found that the temperature in winter polar region in the lower thermosphere increases during SSW events. This is related to upward propagation of the planetary wave excited in the mesosphere.

Keywords: stratospheric sudden warming, mesosphere, lower thermosphere

Japan Geoscience Union Meeting 2014
(28 April - 02 May 2014 at Pacifico YOKOHAMA, Kanagawa, Japan)

PEM36-P03 Room:Poster Time:April 28 18:15-19:30

Vertical profiles of atmospheric temperature between upper troposphere and mesosphere obtained from Rayleigh/Raman lidar

NISHIYAMA, Takanori[1*] ; NAKAMURA, Takuji[1] ; EJIRI, Mitsumu[1] ; ABO, Makoto[2] ; KAWAHARA, Taku d[3] ; TSUDA, Takuo[1] ; SUZUKI, Hidehiko[4] ; TSUTSUMI, Masaki[1] ; TOMIKAWA, Yoshihiro[1]

[1]National Institute of Polar Research, [2]Graduate School of System Design, Tokyo Metropolitan University, [3]Faculty of Engineering, Shinshu University, [4]Faculty of Science, Rikkyo University

Atmospheric gravity waves (AGWs) propagating upward from lower atmospheric sources play a dominant role in transportating and depositing energy and momentum from upper troposphere (UT) to lower mesosphere (LM). Particularly, in polar region, these effects of AGWs are well-known to strongly decelerate the polar night jet and drive large scale meridional circulation from the summer pole towards the winter pole. In addtion, it is suggested that considerations of the realistic propagation property of AGWs may largely improve a significant bias of climate model. Therefore, investigation of the activity of AGWs between UT and LM based on continuous observational studies can be regarded as one of important isuues.

The National Institute of Polar Research (NIPR) is leading a six year prioritized project of the Antarctic research observations since 2010. One of the sub-projects is entitled 'the global environmental change revealed through the Antarctic middle and upper atmosphere'. As a part of the sub-project, a Rayleigh/Raman lidar (RR lidar) was installed at Syowa, Antarctica (69S, 39E) in January, 2011. The operation has been conducted since February 2011 and the RR lidar has kept measuring temperature profiles continuously between approximately 10 and 80 km for almost 3 years.

The RR lidar system in Syowa can obtain photon count data for 4 channels simultaneously, and each data is recorded separately in binnary format. The data from 3 channeles, i.e., Raman (10-30km), Rayleigh-Low (20-65km), Rayleigh-High (30-80km), corresponding to differenet height ranges are used for estimations of temperature profiles from UT to LM. In oreder to estimate height continuous profiles of atmospheric temperature based on the 3 different channeles, we are examing the following analysis methods. (1) The temperature for Rayleigh-High and Rayleigh-Low channels estimated by solving the lidar equation can be assigned to temperature at an initial height for the lidar equation in Rayleigh-Low and Raman channels, respectively. (2) The initial heights for the lidar equation can be determined automatically taking into account time and height dependent shot noises due to background luminosity. (3) The error propagations from the initial height to lower heights are evaluated by assigning artificial temperature offset ranging from -50 to 50 K.

The height continuous temperature profiles between UT and LM obtained from improved analysis methods would allows us to investigate important scientific issues such as temporal and height variabilities of potential energy per unit mass of AGWs and the relationship between occurrence of Polar Stratospheric Clouds and background atmospheric temperature. In this presentation, we will report the detail of the analysis methods and future perspectives including open data base of temperature profiles.

Keywords: Rayleigh/Raman lidar, Atmospheric temperature, Mesosphere, Stratosphere, Atmospheric Gravity Waves, Polar Stratospheric Clouds

Japan Geoscience Union Meeting 2014
(28 April - 02 May 2014 at Pacifico YOKOHAMA, Kanagawa, Japan)

PEM36-P04 Room:Poster Time:April 28 18:15-19:30

Tunable resonance scattering lidar system for Antarctic observation: Current status

TSUDA, Takuo[1*] ; EJIRI, Mitsumu[1] ; NISHIYAMA, Takanori[1] ; ABO, Makoto[2] ; MATSUDA, Takashi[1] ; KAWAHARA, Takuya[3] ; NAKAMURA, Takuji[1]

[1]National Institute of Polar Research, [2]Graduate School of System Design, Tokyo Metropolitan University, [3]Faculty of Engineering, Shinshu University

We are developing a new resonance scattering lidar system to be installed at Syowa Station (69S, 39E) in Antarctica. For the new lidar system, we have employed a tunable alexandrite laser covering the resonance scattering wavelengths of two neutral species, which are atomic potassium (K, 770.11 nm) and atomic iron (Fe, 386.10 nm), and two ion species, which are calcium ion (Ca^+, 393.48 nm) and aurorally excited nitrogen ion ($N_2{}^+$, 390.30 nm, 391.08 nm). Thus the tunable resonance scattering lidar system will provide information on the mesosphere and lower thermosphere as well as the ionosphere. Using the tunable lidar and co-located other instruments, we will conduct a comprehensive ground-based observation of the low, middle, and upper atmosphere above Syowa Station. This unique observation is expected to make important contribution to studies on the atmospheric vertical coupling process and the neutral and charged particle interaction. In this presentation, we report current status of the tunable lidar system in development and test observations at National Institute of Polar Research in Tachikawa, Japan.

Keywords: Resonance scattering lidar, Antarctica, Syowa Station, K layer, Fe layer

Japan Geoscience Union Meeting 2014
(28 April - 02 May 2014 at Pacifico YOKOHAMA, Kanagawa, Japan)

PEM36-P05 Room:Poster Time:April 28 18:15-19:30

Doppler-free spectroscopy experiments for the Antarctic Potassium resonant lidar

KAWAHARA, Takuya[1] ; TSUDA, Takuo[2*] ; NISHIYAMA, Takanori[2] ; EJIRI, Mitsumu[2] ; ABO, Makoto[3] ; NAKAMURA, Takuji[2]

[1]Faculty of Engineering, Shinshu University, [2]National Institute Polar Research, [3]System Design, Tokyo Metropolitan University

The National Institute of Polar Research (NIPR) is leading a six year prioritized project of the Antarctic research observations since 2010. One of the sub-projects is entitled ”the global environmental change revealed through the Antarctic middle and upper atmosphere”. Profiling dynamical parameters such as temperature and wind, as well as minor constituents is the key component of observations in this project, together with long-term observations using existent various instruments in Syowa, the Antarctic (39E, 69S). As one of the instruments in this project, a new resonance scattering lidar system with tunable wavelengths is developed to be installed and operated at the Syowa Station. The lidar transmitter is based on injection-seeded, pulsed alexandrite laser for 768-788 nm (fundamental wavelengths) and a second-harmonic generation (SHG) unit for 384-394 nm (second harmonic wavelengths). In order to tune the seeder laser to absolute Potassium resonance line, Doppler-free spectroscopy with a Potassium cell is crucial. The measurement was done at NIPR and the Doppler-free spectrum was recorded with 0.005 pm wavelength resolution. Three absorptions spaced with 0.05pm at the cross-over wavelength were clearly measured. In this talk, details of the experiment will be shown.

Keywords: Antarctica, lidar, Potassium, resonant scattering, Doppler Free

Japan Geoscience Union Meeting 2014
(28 April - 02 May 2014 at Pacifico YOKOHAMA, Kanagawa, Japan)

PEM36-P06 Room:Poster Time:April 28 18:15-19:30

Development of a 3D sodium lidar: synchronous experimentation and validation

MURANAKA, Wataru[1*] ; KAWAHARA, Taku d[2] ; NOZAWA, Satonori[3]

[1]GSI, Shinshu University, [2]Faculty of Engineering, Shinshu University, [3]STE Lab., Nagoya University

Shinshu University, Nagoya University and RIKEN developed an all solid-state, high-power Na lidar for the temperature/wind measurements in the MLT region over EISCAT radar site in Tromso (69 N), Norway. Current observation is five-direction mode applied to the fixed direction such as vertical and 30 degree tilted to the north, south, east and west from the vertical.

We are now updating the lidar to multi-direction system which has never been done with resonant lidars. The transmission system uses two mirrors with electric rotary stages to emit laser light to any direction of the sky. Receiver system uses a telescope controlled by a PC. The coordination of the telescope is done with direction of so me blight stars. This repeatability pointing to the same direction is 5.3 mrad.

In this talk, we will discuss the experimental results of the synchronized experiments with the laser direction and telescope field-of-view.

Keywords: sodium, lidar, three diminutional

Japan Geoscience Union Meeting 2014
(28 April - 02 May 2014 at Pacifico YOKOHAMA, Kanagawa, Japan)

PEM36-P07 Room:Poster Time:April 28 18:15-19:30

Analysis of the factors of seasonal variation of the thermosphere-mesosphere NO observed at Syowa Station

UEMURA, Miku[1] ; ISONO, Yasuko[1] ; MIZUNO, Akira[1] ; NAGAHAMA, Tomoo[1] ; EJIRI, Mitsumu K.[2] ; TSUTSUMI, Masaki[2] ; NAKAMURA, Takuji[2*]

[1]Solar-Terrestrial Environment Laboratory, Nagoya University, [2]National Institute of Polar Research

When high-energy particles such as solar protons and energetic electrons fall down to the earth's atmosphere, the nitrogen oxides (NO, NO2) are increased in the mesosphere and the upper stratosphere in the polar regions (e.g. Lopez-Puertas et al. 2005). In collaboration with the National Institute of Polar Research, Nagoya University Solar-Terrestrial Environment Laboratory installed a millimeter-wave spectroscopic radiometer at Syowa Station in Antarctica. We have conducted continuous observation of the NO spectrum since January 2012. The NO column density derived from this observation shows a seasonal variation that the NO column density increases up to about 1.7×10^{15} cm^{-2} in winter and decreases down to about 0.5×10^{15} cm^{-2} in summer. In order to understand the mechanism of the seasonal variation, we compared it with seasonal variation of CO vertical distribution in thermosphere-mesosphere and the length of sunshine hours at Syowa Station. Since CO photochemical lifetime is longer than or equal to the horizontal and vertical transport in the thermosphere and the stratosphere, CO can be considered as a good tracer of atmospheric transport. We used CO data obtained by AULA / MLS (Version3.3).

The CO volume mixing ratio in a latitude range of 65 S-75 S and an altitude range of 0.1-0.01 hPa shows a tendency that the mixing ratio increased in winter and decreased in summer. The peak altitude of the mixing ratio changed from upper altitude to lower altitude during winter, suggesting downward transport of the atmosphere. The commencements of the increment of the NO column density and the CO mixing ratio were almost coincident, but the temporal variation patterns of NO and CO did not agree well with each other especially in the decrement phase. On the other hand, the temporal variation pattern of the NO column density and the length of night time showed good correlation throughout the period during which the NO enhancement was significant. Thus the variation of the NO column density in the lower thermosphere-mesosphere is considered to be caused by both the descending of the air mass and the photochemical process.

In this poster, we will present more detailed discussion on the relationship among the NO column density, CO mixing ratio, and length of the night time based on the dataset including the new data acquired this year.

Keywords: microwave spectroscopy, Nitric Oxide

Japan Geoscience Union Meeting 2014
(28 April - 02 May 2014 at Pacifico YOKOHAMA, Kanagawa, Japan)

PEM36-P08 Room:Poster Time:April 28 18:15-19:30

Small spatial scale field aligned currents in middle and low latitudes as observed by the CHAMP satellite

NAKANISHI, Kunihito[1*] ; IYEMORI, Toshihiko[1] ; AOYAMA, Tadashi[1] ; LUHR, Hermann[2]

[1]Department of Geophysics, Graduate School of Science, Kyoto University, [2]GeoForschungsZentrum, GFZ, Potsdam, Germany

The magnetic field observation by the CHAMP satellite shows the ubiquitous existence of small scale (1-5 nT) magnetic fluctuations with period around a few tens seconds along the satellites. From characteristics of the amplitude and period, they can be interpreted as the spatial structure of small scale field-aligned currents generated by the ionospheric dynamo driven by atmospheric gravity waves propagating from the lower atmosphere. The mechanism is the following; first, the gravity waves generated by the lower atmospheric disturbance propagate to the ionosphere; the neutral winds oscillate, cause ionospheric dynamo and Pedersen and Hall currents flow; because the dynamo region is finite, the currents cause polarized electric fields; and the polarized electric fields propagate along the geomagnetic filed as Alfven waves accompanied by field-aligned currents, at the same time, the ionospheric currents divert to the filed aligned currents; finally the CHAMP satellite observes the spatial structure of the filed aligned currents generated in this way as a temporal change along the path, because the temporal variation of the gravity waves are slow enough, i.e., more than a few minutes, that is, that of field aligned current can be ignored and nearly constant for the satellite crossing the currents.

This time we analyze correlation relation of the two components perpendicular to the geomagnetic field to find the following tendencies. About the magnetic data at the observed point, 1) if inclination and declination are plus and plus respectively, a correlation coefficient tends to be minus; 2) if inclination and declination are plus and minus respectively, it tends to be plus; 3) if inclination and declination are minus and plus respectively, it tends to be plus; 4) if inclination and declination are minus and minus respectively, it tends to be minus.

We report the model of the current system consistent to the characteristics of the magnetic fluctuations including the tendency of the correlation relation.

Keywords: spatial structure of field aligned currents, middle and low latitudes, the CHAMP satellite, atmospheric gravity wave, the lower atmospheric origin, correlation relation

Japan Geoscience Union Meeting 2014
(28 April - 02 May 2014 at Pacifico YOKOHAMA, Kanagawa, Japan)

PEM36-P09 Room:Poster Time:April 28 18:15-19:30

Atmospheric origin of small-scale magnetic fluctuations as observed by CHAMP above the ionosphere

AOYAMA, Tadashi[1*] ; IYEMORI, Toshihiko[2] ; NAKANISHI, Kunihito[1]

[1]Graduate School of Science, Kyoto University, [2]Graduate School of Science, Kyoto University

We analyzed magnetic field data obtained by a LEO(Low Earth Orbit) satellite, CHAMP(altitude 300˜450 km), and found out the global distribution of the short-period(10˜40 s) and small-amplitude(0.1˜5 nT) magnetic fluctuations in middle and low latitudes. We have reported that these fluctuations are small-scale structure(˜100 km) of the field-aligned currents generated by dynamo action in the ionospheric E-layer and the dynamos are caused by the atmospheric gravity waves (horizontal scale is ˜100 km) because of the characteristics of geographical and seasonal dependence of their amplitude.

In this paper, we focus on the mesoscale meteorological events to clarify the atmospheric origin such as typhoon which is possible to generate atmospheric gravity waves, and compare with magnetic fluctuations as observed by the CHAMP satellite above the ionosphere. We trace from the location of CHAMP to each footpoint in the E-layer along geomagnetic field line, and then compared with meteorological phenomena beneath the footpoint.

As a result, we detected large amplitudes of geomagnetic fluctuation above typhoons.

Keywords: field-aligned current, ionospheric dynamo, atmospheric gravity wave, acoustic resonance, CHAMP satellite, typhoon

Japan Geoscience Union Meeting 2014
(28 April - 02 May 2014 at Pacifico YOKOHAMA, Kanagawa, Japan)

PEM36-P10 Room:Poster Time:April 28 18:15-19:30

Optimization of notification system for bright meteor signals by using wide angle images at multiple sites

IYONO, Atsushi[1*] ; WADA, Naoki[2]

[1]Dept. of Fundamental Science, Okayama university of Science, [2]Graduate School of Science, Okayama university of Science

1. Purpose and Background

The sky monitoring system by using wide angle images have been maintained until Nov. 2011 at Okayama University of Science. The CCD camera system provides the slow shutter images every 3 second, and they have been transferred simultaneously to data storage server via the Internet connection. This system enables to monitor the real time condition of the sky. In the obtained images, bright meteors and sometimes fire balls were registered. We have been developing our new system which can provide quick analysis results for meteor and fire ball at the moment of observations. In this report, we describe the new sensor systems of thermography and low frequency sounds to increase the detection efficiency of brighter meteors and fire balls.

2. System

In the sky monitor system, CCD camera with wide angle lens and image server system have been operated in 24 hours/day. The exposure of CCD cameras has been set to be 4 second. The acquired image data have been stored in PC system via the internet ftp command. 28,800 images(500MB data

size) are stored in each day. In offline mode, images are processed with contrast enhancement module, image differentiating and object detection module. To detect meteors and fire balls effectively, we activated the IR image seosors and low frequency sound sensors as well as imaging devices.

3. Development

Our purposes are that new analysis system for online processing of images, IR sensors and low frequency seonsors have been developed in order to provied the information of the arrival of meteor and fireballs, arrival directions and brightness profiles. We are going to present new system and analysis result in this reports

Keywords: meteor, fireball, simultaneous? observation, meteor shower

Japan Geoscience Union Meeting 2014
(28 April - 02 May 2014 at Pacifico YOKOHAMA, Kanagawa, Japan)

PEM36-P11 Room:Poster Time:April 28 18:15-19:30

Measurement of propagation characteristics of MF band radio waves in lower ionosphere by S-310-40 sounding rocket

ISHISAKA, Keigo[1*] ; ITAYA, Keita[1] ; ASHIHARA, Yuki[2] ; ABE, Takumi[3] ; ENDO, Ken[4] ; KUMAMOTO, Atsushi[4]

[1]Toyama Prefectural University, [2]NARA National College of Technology, [3]ISAS/JAXA, [4]Tohoku University

The ionospheric D region is important in radio wave propagation because it absorbs energy from waves at MF, HF and VHF, and it reflects LF and VLF signals. Then D region is present only during daylight hours. Therefore, in the night-time, the MF band radio waves are propagated as far as an area where its radio waves cannot be propagated in the daytime. This reason why the radio waves cannot receive is that the D region is disappeared at night. However, the MF band radio waves that transmit from distant place have not been often received at the mid latitude in the night-time. In this time the sporadic E region cannot be observed by the ionogram. We guess that the D region appear in the lowest ionosphere like a daytime. To farther study the structure of the lowest ionosphere, we propose a method to measure the very low electron densities that occur at altitudes from 50 km to 90 km using the partial and perfect reflection characteristics of electromagnetic waves.

S-310-40 sounding rocket experiment was carried out at Uchinoura Space Center (USC) at 23:48 JST on 19 December, 2011. The purpose of this experiment is the investigation of characteristics of radio wave propagation in the ionosphere and the estimation of electron density structure in the lower ionosphere, when the intensity of radio wave measured on the ground will be attenuate at night-time. In order to measure the radio waves, a LF/MF band radio receiver (LMR) is installed on the sounding rocket. The LMR has measured the propagation characteristics of four radio waves at frequencies of 60 kHz (JJY signal from Haganeyama radio station), 405 kHz (NDB station from Minami-Daito), 666 kHz (NHK Osaka broadcasting station) and 873 kHz (NHK Kumamoto broadcasting station) in the region from the ground to the lower ionosphere. The LMR consists of a loop antenna, a pre-amplifier and a detector circuit. The loop antenna is set up in the nose cone, which is transparent to the LF/MF band radio waves, and is not deployed during the flight. Therefore, the LMR can measure the relative attenuation of radio waves from the ground up to the ionosphere. Furthermore the loop antenna consists of three loop antennas in order to measure three components of four radio waves. Then we can obtain the propagation directions of radio waves in the ionosphere directly.

A propagation vector can be obtained from the propagation characteristic of radio wave. It is possible to estimate electron density profile from a propagation vector, because the propagation vector is dependent on the electron density profile in the radio wave propagation region. We have estimated the electron density profile by the propagation vector. When the electron density profile estimated by the propagation vector was compared with the electron density profile measured with the Langmuir probe and the impedance probe onboard the S-310-40 sounding rocket, it was found that electron density becomes the maximum at an altitude of 104 km.

We show the results of propagation characteristics of radio waves in the ionosphere and explain the propagation vector of radio wave in the ionosphere. And the electron density profile in the ionosphere can be estimated by the propagation vector. We will show the result that it is investigated the influence the lowest ionosphere region has on a MF band radio wave in this study.

Keywords: ionosphere, propagation characteristic of radio wave, rocket experiment

Japan Geoscience Union Meeting 2014
(28 April - 02 May 2014 at Pacifico YOKOHAMA, Kanagawa, Japan)

PEM36-P12 Room:Poster Time:April 28 18:15-19:30

Measurement of LF Standard-Frequency Waves JJY along the track of Shirase during JARE55: Preliminary Report

KITAUCHI, Hideaki[1*] ; NOZAKI, Kenro[1] ; ITO, Hiroyuki[1] ; KONDO, Takumi[1] ; TSUCHIYA, Shigeru[1] ; IMAMURA, Kuniyasu[1] ; NAGATSUMA, Tsutomu[1]

[1]NICT

We developed a highly sensitive, reliable receiving system for the purpose of reception of low frequency (LF) radio waves. The system consists of digital lock-in amplifiers and crossed-loop antennas. Digital lock-in amplifier (DLA) employs phase-sensitive detection (PSD) of periodic signal multiplied by the input reference source of the known signal frequency. This makes it possible to realize very narrow bandpass filter around the reference frequency, detecting/measuring that of very weak signal even in noisy environment. The antenna, on the other hand, consists of orthogonally crossed, larger double loops (receivers R_X, R_Y) and smaller doubles (transmitters T_X, T_Y): the former receivers R_X, R_Y receive LF radio signals of x-, y-components, the latter transmitters T_X, T_Y transmit an instant, weak signal from each x-, y-component for self calibration purpose. The self calibration test is performed by transmitting a weak LF signal for an instant every an hour from the transmitter T_X, T_Y respectively, and receiving this signal from the receivers R_X, R_Y to obtain preassigned field strength. This test indicates if the receivers of the system are working properly and allows us to obtain reliable measurements.

We apply the receiving system to measure the field intensity and phase of the standard frequency and time signals (SFTS) JJY of LF 40 kHz and 60 kHz during the summer expedition of the 55th Japanese Antarctic Research Expedition (JARE), from November 2013 to April 2014. Figure 1 shows temporal evolution of the field intensities JJY 40 kHz (light blue dots) and 60 kHz (brown dots) as well as the self-calibrating radio signals. Our receiving system detects both the LF JJY radio signals even offshore Syowa Station, Antarctic, about 14,000 km away from those transmitting stations. Also the field intensities of the self calibration test show about a consistent preassigned value, assuring the measurements.

Keywords: low frequency (LF) radio waves, call sign JJY of 40 kHz and 60 kHz, standard frequency and time signals (SFTS), self calibration, Japanese Antarctic Research Expedition (JARE), Japanese Antarctic Research Icebreaker Shirase

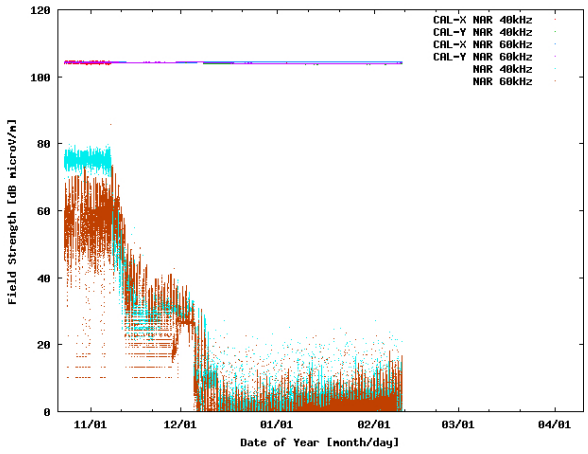

Japan Geoscience Union Meeting 2014
(28 April - 02 May 2014 at Pacifico YOKOHAMA, Kanagawa, Japan)

PEM36-P13 Room:Poster Time:April 28 18:15-19:30

Velocity distribution of electrons generating plasma waves around the wake of an ionospheric sounding rocket

ENDO, Ken[1*] ; KUMAMOTO, Atsushi[1] ; KATOH, Yuto[1]

[1]Department of Geophysics, Graduate School of Science, Tohoku University

When a body moves in plasma at supersonic velocity, a rarefied plasma region called 'plasma wake' is formed behind the body. Wakes can develop behind a solar system body immersed in solar-wind plasma as well as behind spacecraft such as satellites and ionospheric sounding rockets. There are several studies which report plasma waves around the wakes of a satellite and of the moon. Although there are not so many studies which report plasma waves generated in association with the rocket wake, observational results from two rocket experiments performed in 1998 and 2012 have shown generation of plasma waves around the wake of a rocket. It is very important to reveal the generation process of plasma waves near the rocket wake for understanding the universal physics related to the interaction between streaming plasma and a non-magnetized body as well as for interpreting wave data obtained in rocket experiments more accurately.

Our analysis has revealed three kinds of plasma waves observed in the S-520-26 rocket experiment in 2012. They are likely to be electrostatic electron cyclotron harmonic (ESCH) waves, upper hybrid resonance (UHR) mode waves, and whistler mode waves. They have spin-phase dependence in characteristic manners. These results indicate that the plasma waves should be generated inhomogeneously around the rocket. We have performed numerical calculations of plasma dispersion relations by assuming anisotropic velocity distribution functions such as electron beam and temperature anisotropy. As a result, positive linear growth rates have been obtained in the wave number and frequency ranges of UHR mode waves and ESCH waves in addition to electrostatic whistler mode waves. Accordingly, there have to be electrons with some anisotropic velocity distribution functions which are equivalent to those we assumed in the calculations. However, we have to clarify what kind of velocity distribution can be generated around the actual wake through the interaction between a sounding rocket and ionopsheric plasma.

Singh et al. (1987) has performed a one-dimensional simulation of plasma entering a void region from the two sides using a Vlasov-Poisson code. They have found counterstreaming electron beams in the very near wake. However, their study concentrates on electrons on the wake axis and does not indicate distribution functions in other areas. Besides, temperature anisotropy could not be treated in their simulation because it is performed in one dimension in velocity space.

In order to investigate inhomogeneity of electron distribution functions around the rocket wake, we are developing a Vlasov-Poisson code with one-dimensional space and two-dimensional velocity space, which is redesigned from the simulation code used in Singh et al. (1987). In this simulation, we deal with cases that electrons and ions are filling in a void space. The time evolution can be understood as spatial distribution along the wake axis. The direction of one-dimensional space is along the geomagnetic fields, along which electrons and ions can move easily. The size of space is 10 m, which is divided into 1024 grids in the calculation.

In this presentation, we clarify the frequency range and spatial distribution of the plasma waves around the wake based on the analyses of S-520-26 rocket experiment data. We also discuss the velocity distribution of the electrons which can generate the plasma waves as observed. In addition, we report initial results of our simulation for investigating the velocity distribution of electrons around the wake.

Keywords: ionosphere, sounding rocket, wake, plasma wave, Vlasov simulation

Japan Geoscience Union Meeting 2014
(28 April - 02 May 2014 at Pacifico YOKOHAMA, Kanagawa, Japan)

PEM36-P14 Room:Poster Time:April 28 18:15-19:30

Atmospheric Neutral Analyzer for mass-resolved velocity distribution measurements: Verification of mass analyzer

SHIMOYAMA, Manabu[1*] ; HAYASHI, Ayuko[1] ; ITO, Fumihiro[1] ; HIRAHARA, Masafumi[1]

[1]STEL, Nagoya University

In order to understand the temporal and spatial variability of the ionosphere-thermosphere system, simultaneous measurements of the composition and density of the neutral atmosphere and the velocity distribution of individual species are essential. However, most conventional types of instruments for neutral atmosphere lack the simultaneous capability of measuring neutral atmospheric velocity and resolving neutral mass.

We have designed the Atmospheric Neutral Analyzer (ANA) instrument to measure the detailed, mass-resolved 2-dimensional velocity distribution of neutral species, from which the corresponding density, mass composition, bulk velocity and temperature were derived. In this presentation, we will report the results from laboratory experiments for the performance verification on the prototype of mass analyzer along with the detailed and overall design determined by numerical simulation.

Keywords: neutral upper atomosphere, velocity distribution function, mass analysis

Japan Geoscience Union Meeting 2014
(28 April - 02 May 2014 at Pacifico YOKOHAMA, Kanagawa, Japan)

PEM36-P15 Room:Poster Time:April 28 18:15-19:30

Observation of resonance scattering light of Lithium vapor under daytime and moonlight condition and neutral wind analys

KIHARA, Daiki[1*] ; KAKINAMI, Yoshihiro[1] ; YAMAMOTO, Masa-yuki[1] ; WATANABE, Shigeto[2] ; HARD, Lucas[3] ; LARSEN, Miguel[3] ; YAMAMOTO, Mamoru[4] ; HABU, Hiroto[5] ; ABE, Takumi[5]

[1]Kochi Univ. of Tech., [2]Hokkaido Univ., [3]Clemson Univ., [4]Kyoto Univ., [5]ISAS/JAXA

1.Introduction

For the purpose of measurement of neutral atmospheric wind in lower thermosphere, we observed resonance scattering light of sunlit Lithium vapor released from a sounding rocket in the evening thermosphere in 2007 (e.g. Yamamoto et al., 2008). At that time, we successfully measured thermospheric neutral wind profile between 110 km and 400 km. In 2012, we observed resonance scattering light of sunlit Lithium at dawn, and estimated lower thermospheric neutral wind between 76 km and 127 km.

On July 4, 2013, a U.S.-Japan collaborative rocket experiment to observe neutral wind profile in daytime lower thermosphere with Lithium release was carried out at WFF (Wallops Flight Facility), NASA. A rocket to operate chemical release of Lithium was launched at 10:31:40 EDT (14:31:40 UTC). The rocket launched to southeastern direction released Lithium vapor three times between at about 90 km and 130 km altitude during the upleg, at about 40 km horizontally away from a ground-based observation site in WFF. Here we tried to observe of Lithium clouds from the ground-based and airborne observations with collaboration of Kochi University of Technology (KUT) and Clemson University.

On July 20, 2013, a rocket experiment to observe neutral wind profile in moonlit lower thermosphere with Lithium release was carried out at USC (Uchinoura Space Center), Japan. The S-520-27 rocket to operate chemical release of Lithium was launched at 23:57:00 JST and released Lithium vapor three times between at about 80 km and 120 km altitude during the downleg under the almost full moon condition (Moon age was 12). Here we tried to observe of Lithium clouds from 3 ground-based sites and an airplane.

2.Observations

Airborne observation of Lithium cloud was carried out under a condition with the sun at the backward direction while it flew to north-northeast at about 10 km (33,000 feet) altitude and at about 300 km away from the ground site at the southeastern direction. An observation site was set in WFF on ground. In order to detect the Lithium clouds in daytime skies with good S/N ratio, digital cameras (Canon EOS Kiss X4, Nikon D90) with 2 nm band pass filters (BPF) at 671 nm wavelength were used for all digital cameras. We installed three digital cameras in the aircraft NASA-8 and set two digital cameras on the ground site. A video camera (Watec, WAT-120N) with a 12 nm BPF was also used in the aircraft and on ground, respectively.

The Lithium clouds under moonlight condition was observed by using digital cameras, Watec, and cooled EM-CCD (BITRAN BQ-87EM) with 2 nm and 12 nm BPF from the JAXA airplane Hisyo as well as three ground-based observation sites (USC, Tanegashima and Muroto).

3.Results

A Lithium cloud under daytime sky condition was observed for about 25 minutes from the aircraft. The released Lithium vapor formed red clouds along the rocket trajectory just after the release. Afterwards, the Lithium trails were spread into complex shapes by strong wind shear in the altitude. We successfully observed Lithium clouds by the airborne observation.

A Lithium cloud under moonlight sky condition was observed for about 90 seconds from the aircraft and two ground sites.

4.Summary

We successfully observed 2 chemical releases of Lithium from the aircrafts and ground sites on July, 2013, in daytime and midnight. We succeeded the detection of resonance scattering light of Lithium vapor under daytime and moonlight sky condition in lower thermosphere. Owing to this experiment, we confirmed that we can measure altitude profile of the neutral atmospheric wind in lower thermosphere at almost all local time by using the chemical release of Lithium.

In this paper, we will discuss that the observed emission intensity of the resonance scattering light of Lithium vapor under daytime and moonlight sky condition in lower thermosphere, obtained results of the S/N ratio, preliminary results and problems of the neutral atmospheric wind measurement in daytime lower thermosphere.

Keywords: sounding rocket, thermosphere, neutral wind, Lithium Ejection Systems, airborne observation

Japan Geoscience Union Meeting 2014
(28 April - 02 May 2014 at Pacifico YOKOHAMA, Kanagawa, Japan)

PEM36-P16 Room:Poster Time:April 28 18:15-19:30

Improvement of the method for estimating thermospheric temperature using small FPIs and evaluation of their temperatures

NAKAMURA, Yoshihiro[1*] ; SHIOKAWA, Kazuo[1] ; OTSUKA, Yuichi[1] ; OYAMA, Shin-ichiro[1] ; NOZAWA, Satonori[1]

[1]Solar-Terrestrial Environment Laboratory, Nagoya University

Fabry-Perot interferometer (FPI) is an instrument that can measure the temperature and wind velocity of the thermosphere from the ground through observation of airglow emission at a wavelength of 630.0nm. The Solar-Terrestrial Environment Laboratory (STEL), Nagoya University, has five FPIs as parts of the Optical Mesosphere Thermosphere Imagers. Two of those FPIs, possessing a large aperture etalon (diameter: 116mm), were installed at Shigaraki, Japan in 2000 and in Tromso, Norway, in 2009. The other three small FPIs, using 70-mm diameter etalons, were installed in Thailand, Indonesia, and Australia in 2010-2011. They use highly-sensitive cooled-CCD cameras with 1024-1024 pixels to obtain interference fringes. However, appropriate temperature has not been obtained from the interference fringes using these new small-aperture FPIs. In the present study we aimed to improve the procedure of temperature derivation using these small etalon FPIs, to evaluate the accuracy for obtained temperatures and to perform statistical analysis of the temperature data obtained for 2-3 years.

The FPIs scan the sky in north, south, east, and west directions repeatedly by rotating a light receiving mirror. We determined each center of the laser fringe and sky fringes for north, south, east, and west directions. Then we found that they are slightly a few pixels different depending on the mirror directions. This difference of fringe centers seems to be due to distortion of the optics body, which is caused by the motion of the heavy scanning mirror on top of the optics. Thus, we decided to determine the fringe center for each direction. After this revision, we could make a reliable temperature determination. In this presentation, we show these procedures of temperature derivation and relation between airglow intensity and standard deviations of obtained temperatures as accuracy of temperature derivation. We also discuss effects of the etalon gap drift due to changes in etalon temperature for accuracy of measured thermospheric temperatures and winds.

Keywords: Fabry Perot Interferometers, thermospheric temperature

Japan Geoscience Union Meeting 2014
(28 April - 02 May 2014 at Pacifico YOKOHAMA, Kanagawa, Japan)

PEM36-P17 Room:Poster Time:April 28 18:15-19:30

Statistical characteristics of MSTIDs observed by 630-nm airglow imager and HF-radar echoes at Paratunka, Russia

MINOURA, Takeshi[1*] ; SUZUKI, Shin[1] ; SHIOKAWA, Kazuo[1] ; OTSUKA, Yuichi[1] ; NISHITANI, Nozomu[1] ; HOSOKAWA, Keisuke[2]

[1]Solar-Terrestrial Environment Laboratory, Nagoya University, [2]Department of Communication Engineering and Informatics, University of Electro-Communications

Medium-scale traveling ionospheric disturbances (MSTIDs), which typically have a horizontal scale of 100-500 km and a period of ˜1 h, are frequently observed in the F region ionosphere at middle latitudes. To date, quite a few observations of MSTIDs have been carried out especially in the middle latitudes; they predominantly had a northwest-southeast, (northeast-southwest) frontal structure and propagated southwestward (northeastward) in the northern (southern) hemisphere, however their generation and propagation mechanisms are not clear yet. Suzuki et al. [2009] investigated two dimensional characteristics of a nighttime MSTID using the SuperDARN Hokkaido HF radar at Rikubetsu, (43.5 N, 143.6 E), Japan, and an OI 630-nm airglow imager located at Paratunka (53.0 N, 158.2 E), Russia, within the radar field of view (FOV). The Doppler velocities of MSTID echoes observed by the SuperDARN radar showed systematic polarity changes which were consistent with airglow intensity variations. The electric field estimated from the airglow and SuperDARN observations, however, seems to be improbable and the E-F coupling processes would be important to explain the inconsistency. We investigated statistical characteristics of nighttime MSTIDs. Based on the coordinated airglow and SuperDARN measurements from 2011 to 2013, we investigated the relation between the MSTID amplitudes in the 630-nm airglow intensity and the Doppler velocities of the FAI echoes associated with the MSTID pattern. This study may give an observational insight into the E-F coupling quantitatively.

In this presentation, we will report the statistics of the relation of the FAI echoes and airglow signatures of the observed MSTIDs (5 events), which showed spatially conjugation in the radar FOV.

Keywords: airglow imager, Hokkaido SuperDARN radar, MSTID

Japan Geoscience Union Meeting 2014
(28 April - 02 May 2014 at Pacifico YOKOHAMA, Kanagawa, Japan)

PEM36-P18 Room:Poster Time:April 28 18:15-19:30

Detection of ionospheric disturbances caused by the earthquake using HFD

TAKABOSHI, Kazuto[1*] ; NAKATA, Hiroyuki[1] ; TAKANO, Toshiaki[1] ; TOMIZAWA, Ichiro[2]

[1]Graduate shool of Engineering, Chiba University, [2]Center for Space Science and Radio Engineering,Univ. Electro-Comm

Many studies have reported that ionospheric disturbances occur after giant earthquakes. This is because the acoustic wave and/or atmospheric gravity wave are excited by the ground perturbations or tsunami. The HF Doppler observation is suitable for detection of ionospheric disturbances since this can observe ionospheric vertical drift from Doppler shift of radiowaves (5006 and 8006 kHz) transmitted from the Chofu campus of UEC. In this study, usng Doppler shift data of 5006 kHz, ionospheric disturbances associated with earthquakes are ditected. When Doppler shift is fluctuated intensely after propagation time of Rayleigh wave from the seismic center to the observation points, the fluctuation is determined as a disturbance associated with the earthquakes.

In 55 events of earthquakes (M≥6.0) occurred around Japan since 2003, fluctuations by earthquakes are detected in 14 events and the smallest magnitude is 6.4. No fluctuation is detected in some larger earthquakes than M6.4. Since the ionosphere is unstable at night, received frequency is disturbed and it is hard to determine the fluctuations caused by earthquake. In addition, the observation points are not always located near the seismic centers. When earthquakes occur near observation points at the daytime, it is expected that the fluctuations caused by earthquakes are observed even if the magnitudes of the earthquakes is smaller than M6.4.

We also examined the relationship between direction of fault and fluctuations of HFD data. Most of the earthquakes in Japan are reverse fault type. Because a hanging wall slides up in this type of an earthquake, it is expected that initial perturbation of a sound wave excided by the hanging wall is upward. Actually, in most of the events Doppler shifts are negative, which means that the ionosphere moves upward. Next we examined a normal-fault-type earthquake (Fukushima hama-dori earthquake, 2011/4/11), in which a hanging wall slips down. In this event, the epicenter is located at the east of Fukushima prefecture. Doppler data of three observation points (Iitate, Sugadaira, Kiso) are examined. In Iitate observatory, which is the closest to the epicenter, Doppler data shows that ionosphere moved only upward. On the contrary, in the other two points, Doppler data shows that ionosphere moved downward first and then upward, or upward first and then downward. Therefore, fluctuations of ionosphere can not be determined only by a type of fault. More detailed analysis using the seismometer is necessary.

Keywords: ionosphere, HFD, earthquake, acoustic wave, atmospheric gravity wave, fault

Japan Geoscience Union Meeting 2014
(28 April - 02 May 2014 at Pacifico YOKOHAMA, Kanagawa, Japan)

PEM36-P19 Room:Poster Time:April 28 18:15-19:30

Observations of seismo-traveling ionospheric disturbance during the 2011 Tohoku earthquake using HF Doppler

CHOU, Min-yang[1*] ; TSAI, Ho-fang[1] ; LIU, Jann-yenq[2]

[1]Department of Earth Science,National Cheng-Kung University,Taiwan, [2]Institute of Space Science, National Central University, Taiwan

This paper reports seismo-traveling ionospheric disturbances (STIDs) induced by the 11 March 2011 M9.0 Tohoku-oki earthquake and following pan-Pacific tsunami by two networks of HF (high-frequency) Doppler sounding systems in Japan and Taiwan. The Hilbert-Huang Transform (HHT) is applied to analyze Doppler frequency shifts (DFSs) detecting STIDs, while the time delay, circle, ray-tracing, and beam-forming methods are used to compute the propagation of the detected STIDs. Both STIDs induced by the Rayleigh waves and tsunami of the Tohoku-oki earthquake are detected and discussed.

Keywords: STIDs, Ionosphere, earthquake, tsunami

Japan Geoscience Union Meeting 2014
(28 April - 02 May 2014 at Pacifico YOKOHAMA, Kanagawa, Japan)

PEM36-P20 Room:Poster Time:April 28 18:15-19:30

Spectrum of the neutral atmospheric waces derived from a numerical simulation of an earthquake

SHIMIZU, Yuki[1*] ; NAKATA, Hiroyuki[1] ; TAKANO, Toshiaki[1] ; MATSUMURA, Mitsuru[2]

[1]Grad. School of Eng. , Chiba Univ., [2]Center for Space Science and Radio Engineering, University of Electro-Communications

It is important to examine the ionospheric disturbances excited by earthquakes, since this contributes to monitoring tsunamis from satellites. There are many reports of ionospheric disturbances occurred by giant earthquakes, such as the 2011 off the Pacific coast of Tohoku Earthquake. But characteristics of atmospheric disturbances, connecting the ionospheric disturbances with the ground and the sea surface, is not clarified because broad observation of the atmosphere in high resolution is difficult. In this study, calculating the spectra from the temporal variations of neutral atmospheric waves determined by a numerical simulation, we derived the features of the propagation of the atmospheric waves.

In this simulation, two dimensional model is used. The atmospheric perturbation is created by a vertical velocity assuming an upward motion of the sea surface or ground surface. Calculating the temporal variations of neutral density, we derived their spectra.

As a result, it is shown that behavior of atmospheric waves is different for the frequency. For a notable example, variations around 1 mHz propagate to high altitudes 450 km ˜500 km and long distance 800 km. On the other hand, variations around 10 mHz propagate almost the same distance in lower altitude of 300 km or less. In addition, variation at 4 mHz are located above the epicenter at 350 km. This causes the variation of GPS-TEC at 4 mHz associated with earthquakes that have ever been reported.

Keywords: ionosphere, earthquake, acoustic wave, gravity wave

Japan Geoscience Union Meeting 2014
(28 April - 02 May 2014 at Pacifico YOKOHAMA, Kanagawa, Japan)

PEM36-P21 Room:Poster Time:April 28 18:15-19:30

Ionospheric effects on the F region during the Sunrise for the annular solar eclipse over Taiwan on 21 May 2012

CHUO, Yu-jung[1*]

[1]Department of Information Technology, Ling Tung University

On 21 May (20:56, Universal Time; UT, on 20 May), 2012, an annular solar eclipse occurred, beginning at sunrise over southeast China and moving through Japan, sweeping across the northern Pacific Ocean, and completing its passage over the western United States at sunset on 20 May (02:49 UT, 21 May), 2012. We investigated the eclipse area in Taiwan, using an ionosonde and global positioning system (GPS) satellites measurements. The measurements of foF2, hmF2, bottomside scale height around the peak height (Hm), and slab thickness (B0) were collected at the ionosonde station at Chung-Li Observatory. In addition, we calculated the total electron content (TEC) to study the differences inside and outside the eclipse area, using 3 receivers located at Marzhu (denoted as MATZ), Hsinchu (TNML), and Henchun (HENC). The results showed that the foF2 values gradually decreased when the annularity began and reached a minimum level of approximately 2.0 MHz at 06:30 LT. The hmF2 immediately decreased and then increased during the annular eclipse period. The TEC variations also appeared to deplete in the path of the eclipse and opposite to the outside passing area. Further, the rate of change of the TEC values (dTEC/dt measured for 15 min) was examined to study the wave-like fluctuations. The scale height near the F2 layer peak height (Hm) also decreased and then increased during the eclipse period. To address the effects of the annular eclipse in the topside and bottomside ionosphere, this study provides a discussion of the variations between the topside and bottomside ionospheric parameters during the eclipse period.

Keywords: ionospheric physics, ionospheric disturbances, solar radiation effects

Japan Geoscience Union Meeting 2014
(28 April - 02 May 2014 at Pacifico YOKOHAMA, Kanagawa, Japan)

PEM36-P22 Room:Poster Time:April 28 18:15-19:30

Horizontal shapes of mid-latitude sporadic-E observed with GPS-TEC

MAEDA, Jun[1*] ; HEKI, Kosuke[1]

[1]Graduate school of Science, Hokkaido University.

The horizontal shapes of sporadic-E (Es) have remained uncovered due to the lack of effective observation methods. We use a dense array of Global Positioning System (GPS) receivers in Japan to map horizontal shapes of mid-latitude sporadic-E layers and explore their diversity. The spatial and temporal resolutions of the GPS array are ˜25 km (in horizontal) and 30 s, respectively, which is ideal for studying the horizontal shape and movement of sporadic-E. Sporadic-E can be identified as positive anomalies of total electron content (TEC) along the line of sight between a satellite and a ground-based GPS station.

The results of GPS-TEC observation, i.e., mapping of positive TEC anomaly caused by mid-latitude sporadic E are presented in this presentation with a special emphasis on latitudinal and temporal variations of horizontal shapes of Es-layers. We analyzed ˜100 Es events in 2010-2013 to examine the latitudinal dependence of Es frontal structures with three study areas at different latitudes near ionosondes, namely Sarobetsu (geographical latitude: 45.16 N), Kokubunji (35.71 N) and Yamagwa (31.20 N).

As a result, strong Es shares the large-scale frontal structure as a common shape regardless of the occurrence latitude and time (e.g., morning, afternoon, and the evening). The horizontal structures of large-scale fronts are typically elongated in east-west (E-W) with the length and width of ˜300 km and ˜30 km, respectively. However, lengths vary from 30 to 300 km by occasion. The alignment of frontal structures prefers E-W, ENE-WSW and NE-SW alignment with some exception of NW-SE and NNW-SSE aligned structures.

We will also discuss the possible mechanisms for formation, development, and movement of mid-latitude sporadic-E based on the results of our observations and proposed theories.

Keywords: Sporadic-E, GPS, TEC

Japan Geoscience Union Meeting 2014
(28 April - 02 May 2014 at Pacifico YOKOHAMA, Kanagawa, Japan)

PEM36-P23 Room:Poster Time:April 28 18:15-19:30

GPS-TEC observation using two-frequency software receiver

ASHIHARA, Yuki[1*] ; KOMATSU, Kazuki[1]

[1]Dept. of Electrical Engineering, Nara National College of Technology

Global Positioning System (GPS) is a high accuracy positioning system that uses radio waves transmitted from several GPS satellites. The carrier signals of GPS satellites, there are two frequencies of L1 (1575.42MHz) and L2 (1227.60MHz). In the ionospheric plasma, the refractive index depends on the electron density. In addition, since the plasma is dispersive medium, each of L1 and L2 waves has different refractive indexes. Therefore, it is occurred propagation delay time (phase difference) in between these signals.

GPS-TEC (GPS Total Electron Contents) is a method to obtain the total electron contents along the line of satellite (LOS) from the phase difference between these signals. GPS-TEC is very useful technique to observe ionospheric electron density, but two-frequency GPS receiver is very expensive. Therefore, GPS-TEC has calculated by using GEONET data in most cases in Japan.

In the informatics and communication field, software receiver is being widely for demodulating the baseband signal, as a background of higher performance of computers. In this study, we build a software GPS receiver system, and receive the two-frequency signals. And we will evaluate the GPS-TEC data obtained by this observation.

Keywords: ionosphere, GPS-TEC, software receiver

Japan Geoscience Union Meeting 2014
(28 April - 02 May 2014 at Pacifico YOKOHAMA, Kanagawa, Japan)

PEM36-P24 Room:Poster Time:April 28 18:15-19:30

Total electron content observation by using GPS, QZSS and BeiDou

KINUGASA, Natsuki[1*] ; TAKAHASHI, Fujinobu[1]

[1]Yokohama National University

There are several methods for observation of total electron content (TEC). TEC can be obtained from the measurement of global navigation satellite system (GNSS) such as GPS. Recently, RNSS (regional navigation satellite system) has been developed in China and Japan. We are trying to use RNSS for TEC observation.

RNSS makes TEC observation stable since a satellite is tracked continuously for long time. It is of benefit to study of plasmasphere because the altitude is higher than GNSS. There is also drawback. Since the direction of vector from grand receiver to satellite is not so variable, it is hard to observe the horizontal electron density distribution of ionosphere. This problem can be solved by combining with measurements of RNSS and GNSS. That is called multi-GNSS.

TEC can be caluculated from the difference of delay between dual-frequency. The inter-frequency bias which remain in TEC measurement are required to estimated and removed. We will present model of ionospheric electron density distributionfor the bias estimation procedure. We have constructed the observation system for GPS, Japanese QZSS, and Chinese BeiDou in Yokohama National University. Various observational results will be shown and discussed.

Keywords: TEC, QZSS, BeiDou, GPS, ionosphere, plasmasphere

Japan Geoscience Union Meeting 2014
(28 April - 02 May 2014 at Pacifico YOKOHAMA, Kanagawa, Japan)

PEM36-P25 Room:Poster Time:April 28 18:15-19:30

Total Electron Content prediction model over Japan using an artificial neural network

NISHIOKA, Michi[1*] ; TSUGAWA, Takuya[1] ; MARUYAMA, Takashi[1] ; ISHII, Mamoru[1]

[1]National Institute of Information and Communications Technology

Forecasting Total Electron Content (TEC) is important for Space Weather; for predicting propagation delay of the radio waves in the ionosphere. Although several empirical and theoretical models have been developed, no model is available for forecasting TEC over Japan. Our purpose is to accomplish an operational TEC model over Japan using an artificial neutral network (ANN) technique which is developed by Maruyama [2007]. In our model, absolute TEC values for each day from 27^{o}N to 45^{o}N in latitude and 127^{o}E to 145^{o}E in longitude were projected on a two-dimension TEC map, that is, a local-time and latitudinal map. Then the time-latitudinal variation was fitted by using the surface harmonic function. The coefficients of the expansions were modeled by using a neural network technique. For the learning process, we used absolute TEC value from 1997 to 2013. The input parameters are proxies of the season, the solar activity, and the geomagnetic activity. Thus, daily two-dimensional TEC maps can be obtained for any day when the input parameters are provided. We used input parameters which are available in real-time by some institutes and achieved one-day TEC prediction over Japan.

Keywords: Ionosphere, Total Electron Content, Operational model, artificial neural network

Japan Geoscience Union Meeting 2014
(28 April - 02 May 2014 at Pacifico YOKOHAMA, Kanagawa, Japan)

PEM36-P26 Room:Poster Time:April 28 18:15-19:30

Statistical Analyses of Ionospheric Storms Over 50 Years In Japan

NAKAMURA, Maho[1*] ; KAMOGAWA, Masashi[1]

[1]Dpt. of Phys., Tokyo Gakugei Univ.

Statistical analyses of the ionospheric storms over Japan are carried out based on the long-term observations over 50 years in Japan. While there are many types of ionospheric variations such as ionospheric storms, plasma bubbles, TIDs and so on, ionospheric storms are most large fluctuations of electron density in the ionosphere. In general, the increase of the electron density is termed positive storm and the decrease of it is termed negative storm [1]. The positive storms cause satellite-positioning errors due to the delay of radio propagation and negative storms cause HF radio communication outages due to lowering the maximum usable frequency. Because these two types of ionospheric storms shows different characteristics on the duration, scale, and the seasonal dependences, we analyzed ionospheric storm occurrences using critical frequency of the F2 layer; foF2 obtained from ionograms over 4 observation sites (Wakkanai, Kokubunji, Yamagawa, and Okinawa) operated by National Institute of Information and Communications Technology, Japan (NICT) [2]. We extracted ionospheric storms based on the differences between the daily observation values and the one-month median in Japan for more than 50 years. Extracted storms of each station will be analyzed by the occurrences, duration, seasonal dependence and geomagnetic variations.

References
[1] G. W. Prolss, Ionospheric F-region storms, Vol. 2 of Hand book of Atmospheric Electro- dynamics, CRC Press, 1995.
[2] World Data Center for Ionosphere, http://wdc.nict.go.jp/.

Keywords: ionospheric storms, eritical frequency F2 layer, satelite navigation

Japan Geoscience Union Meeting 2014
(28 April - 02 May 2014 at Pacifico YOKOHAMA, Kanagawa, Japan)

PEM36-P27 Room:Poster Time:April 28 18:15-19:30

Statistical analysis of the Speckle applying the ”Hinode” / XRT

YAMADA, Masanori[1*] ; NOZAWA, Satoshi[1] ; SHIMIZU, Toshifumi[2]

[1]Graduate School of Science and Engineering, Ibaraki University, [2]Institute of Space and Astronautical Science, Japan Aerospace Exploration Agency (ISAS/JAXA)

“ When a charge-coupled device (CCD) image is taken, white noise will appear identically main CCD image. For examlpe, the trajectory of noise is watched like scar, small spot and snowstorm, which is call as spike, unwanted signal, and so on. In this study, noise is called “ Speckle ” . The speclke is due to the particle nature of photon when CCD is hitted by Solar Energitc Particle(SEP) or cosmic ray.
SEPs have high energy of 10 keV - 10 GeV, which are generated by solar flare, coronal mass ejection(CME). This reason is that SEP plays an important role in space weather. When SEPs with hige energy of GeV order will come to earth magnetosphere, low earth orbit (LEO) stellite would be damaged the potential of single events like SEPs effect.

For this reason, this study analyzed Hinode / X-Ray Telescope (XRT) images and detected speckles. Analysis period is from January 2011 to July 2013. As a result speckles were periodic fluctuations and significant increased, when on 00:04 UT March 7 2012, X5.4 Flare occurred.
Number of detected speckles had a time zone is 3 or 4 times as high as before the occurrence of the Flare. In addition periodic fluctuations are synchronized with orbital period. Moreover information of the satellite orbit indicates speckles increases over the High Latitude Zone (HLZ). Although this is suggested SEPs flow in HLZ, there is a region with high geomagnetic latitude, so speckles are caused by charged particles of non-SEPs.

This study reports on detailed consequence. Besides it looks at the correlations between decrease or increase in speckles and information of the satellite orbit or solar activity.

Keywords: Space Weather, SEP, Flare, CME, Hinode/X-Ray Telescope(XRT)

Japan Geoscience Union Meeting 2014
(28 April - 02 May 2014 at Pacifico YOKOHAMA, Kanagawa, Japan)

PEM36-P28 Room:Poster Time:April 28 18:15-19:30

Seasonal-longitudinal dependence of the occurrence of equatorial plasma bubbles obserbed by ISS-IMAP

TAKAHASHI, Akira[1*] ; NAKATA, Hiroyuki[1] ; TAKANO, Toshiaki[1] ; SAITO, Akinori[2]

[1]Chiba University, [2]Kyoto University

Equatorial plasma bubbles (EPBs) are local depletions of the electron density in the ionosphere. Ionospheric irregularities are included in EPBs and cause radio signal scintillation. Recently, reseach on applying GNSS to Air Navigation System has progressed, therefore, it becomes more necessary to investigate the generation mechanism and the morphology of EPBs.

In this study, we analyzed seasonal-longitudinal dependence of the occurrence of EPBs using airglow-images obtained by ISS-IMAP (Ionosphere, Mesosphere, upper Atmosphere, and Plasmasphere mapping).In 630-nm airglow images, EPBs are visualized as black lines. 181 events are selected during 2012/09 - 2013/08. To calculate the longitudinal denpendence of occurence rate, we divide the ionosphere into 36 longitude bins, each 10 degrees wide. Since EPBs are observed at low and middle latitude, the total obserbation time is accumlated when |latitude| $<$30. We calculate the occurrence rate as the number of EPBs detected over the total observation time.

The occurrence rate is high at the African-Atlantic-American regeions in the equinoctial seasons. On the other hand, the occurance rate is also high at American-Pacific resions in summmer, which is not obtained in the previous study, Burke et al. [2004], in which EPBs are detected using plasma density data on DMSP satellite. The altitude of DMSP is 840 km, which is higher than the observation altitude of ISS-IMAP, that is about 250 km. Therefore, it is conceivable that the difference of occurrence rate of EPB is due to the altitude of the observations. This imply that ISS-IMAP observation could detect EPBs not developed to higher altitude.

Based on above, we will present seasonal-longitudinal variability of the Rayleigh-Taylor instability growth rate, contributing the development of EPBs using ionosphere model and other observational data.

Keywords: Equatorial ionosphere, Plasma bubble, airglow, ISS-IMAP